Investigating the effect of a small molecule, Inhibitor of Nuclear Import (INI-43) as a pan-cancer treatment

Shabita Rahman

Thesis presented for the degree of

MSc (Med) in Medical Biochemistry

In the Division of Medical Biochemistry and Structural Biology

Department of Integrative Biomedical Sciences

Faculty of Health Sciences

UNIVERSITY OF CAPE TOWN

July 2023

Declaration

I, Shabita Rahman, hereby declare that the work on which this dissertation/thesis is based is my original work (except where acknowledgements indicate otherwise) and that neither the whole work nor any part of it has been, is being, or is to be submitted for another degree in this or any other university.

I empower the university to reproduce for the purpose of research either the whole or any portion of the contents in any manner whatsoever.

Signature: …… Signed by candidate

Date: ……24 July 2023…….

Acknowledgments

I would like to express my sincere gratitude to the following people:

My supervisor, Prof Virna Leaner for your expertise and continued guidance. A special thank you for always understanding and supporting me as an international student.

My co-supervisor, Dr Pauline van der Watt for your excellent advice and invaluable suggestions every day in the laboratory. Thank you for all the motivation.

A/Prof Denver Hendricks for your constant support and kindness.

Hajira Guzjay, for ensuring everything in the laboratory runs smoothly and for training me in Tissue Culture.

Members of the laboratory, Nonku, Gabriella, Jamie and Arad for all the advice and laughs. A special thank you to Bianca, Raabie'ah and Humaira for your endless support and friendship, both in the laboratory and on the tennis court. Thank you for taking special care of me in Cape Town.

University of Cape Town, for the financial assistance.

My family: mummy, daddy and my brother, Ridwan, thank you for your unconditional love and support. Your belief in me has constantly inspired me. Thank you for always being my biggest fans and loudest cheerleaders.

My husband, Nabhan for your love, support and friendship, and for always being interested to learn more about my research.

Abbreviations

BCA	Bicinchonic Acid
BSA	Bovine Serum Albumin
CAS	Cellular Apoptosis Susceptibility
CC_{50}	50% cytotoxic concentration
CETSA	Cellular Thermal Shift Assay
CO_2	Carbon Dioxide
CRM1	Chromosome maintenance 1
CSE1	Chromosome segregation 1-like
°C	Degrees Celsius
DMEM	Dulbecco's modified Eagles Medium
DMSO	Dimethyl Sulphoxide
E6	Oncoprotein
E7	Oncoprotein
EGA	European Genome-Phenome Archive
FCS	Fetal calf serum
GAPDH	Glyceraldehyde 3-phosphate dehydrogenase
GDP	Guanosine diphosphate
GTP	Guanosine triphosphate
GEO	Gene Expression Omnibus
GST	Glutathione transferase
GTEx	The Genotype-Tissue Expression project
INI-43	Inhibitor of Nuclear Import 43

IPO5	Importin 5
KM	Kaplan Meier
KPNα2	Karyopherin alpha 2
KPNβ1	Karyopherin beta 1
MTT	3’-(4’,5’-DDimethylthiazol-2’-yl)2’,5’-diphenyltetralolium
NE	Nuclear envelope
NES	Nuclear Export Signal
nFAT	Nuclear factor of activated T cells
NLS	Nuclear Localisation Signal
NPC	Nuclear Pore Complex
PBS	Phosphate buffered saline
PMA	Phorbol-12-Myristate-13-acetate
RIPA	Radioimmunoprecipitaion assay buffer
rpm	Revolutions per minute
SDS-PAGE	Sodium dodecyl sulphate poly acrylamide gel electrophoresis
SEM	Standard Error of Mean
SINE	Selective Inhibitor of Nuclear Export
siRNA	Small interfering ribonucleic acid
SLS	Sodium Lauryl Sulphate
TBST	Tris Buffered Saline Tween-20
TCGA	The Cancer Genome Atlas
TI	Therapeutic Index
TNPO1	Transportin 1

Units

µg	microgram
mg	milligram
g	gram
µM	micromolar
mM	millimolar
M	molar
µl	microliter
ml	millilitre
L	litre

CONTENTS

Abstract

Karyopherin beta 1 (KPNβ1) is a nuclear import protein that transports cargo molecules from the cytoplasm into the nucleus and plays an important role in other cellular processes such as mitosis and mitotic spindle assembly, DNA replication and cell cycle progression. Previous studies in our laboratory reported that KPNβ1 is overexpressed in cervical and oesophageal cancer and is important for cancer cell survival and function, suggesting that inhibiting KPNβ1 may be a potential targeted anti-cancer strategy. An *in silico* screen identified a small molecule inhibitor, Inhibitor of Nuclear Import (INI-43) as an inhibitor of KPNβ1-mediated nuclear import and showed anti-cancer effects against cervical and oesophageal cancer cells using both cell culture and animal models. In this study, we expanded our investigations by determining KPNβ1 expression using bioinformatic analyses and Western blotting, and by investigating the effects of INI-43 in multiple cancer types grown in cell culture to ascertain the potential of KPNβ1 as a pan-cancer therapeutic target. In addition, we determined the ability of INI-43 to interact with KPNβ1 using a biophysical assay – the Cellular Thermal Shift Assay (CETSA).

Bioinformatic analyses using patient data revealed that KPNβ1 mRNA was significantly overexpressed in multiple cancer tissue compared to non-cancer tissue, including breast cancer, colon cancer, lung cancers and uterine cancers. Interestingly, we also found that more than 50% of the cancers, for which bioinformatic data was available, show poorer patient survival when KPNβ1 is highly expressed. *In vitro* analysis using Western blotting on chosen cultured cell lines of different tissue origin revealed that KPNβ1 is highly expressed in multiple cancer types at the proteomic level, including liver cancer, gastric cancer, osteosarcoma and fibrosarcoma. These results suggest that KPNβ1 is a promising diagnostic/prognostic marker for a broad range of cancer types.

Cancer cell lines of different tissue origin were found to be more sensitive to INI-43 treatment compared to the non-cancer epithelial cell line (ARPE-19) with CC_{50} values ranging between 5

- 15 µM for the cancer cell lines and approximately 25 µM for the non-cancer cell line, ARPE-19, which is at least two to five-fold higher than the CC_{50} values of majority of the cancer cell lines. INI-43 treatment also resulted in cancer cell death by apoptosis as observed by Caspase activity. These results support that INI-43 has potential as a pan-cancer therapeutic agent for multiple cancer types.

To investigate KPNβ1:INI-43 interactions in living cells, we analysed thermal melt profiles of treated and untreated KPNβ1 using the biophysical assay, CETSA. Our study found that treatment with INI-43 has a stabilising effect on KPNβ1, suggesting that INI-43 physically binds to KPNβ1. Furthermore, we obtained data to show that INI-43 does not appear to bind to other nuclear transport proteins that are associated with cancer, including CAS, CRM1, KPNα2, TNPO1 and GAPDH (control). Interestingly, we found that INI-43 appears to bind to another nuclear import protein, IPO5.

In conclusion, this study shows that KPNβ1 is expressed at high levels in multiple cancer types of different tissue origin and that INI-43, a small molecule inhibitor with anti- KPNβ1 activity, has potential as a pan-cancer treatment. The study also provides evidence that INI-43 interacts with KPNβ1 in living cells. These results support that KPNβ1 is a potential anti-cancer therapeutic target for multiple cancer types.

Chapter 1

Literature Review

1.1 Cancer

Cancer is one of the leading causes of death globally, and results from the transformation of normal cells into cancer cells that divide uncontrollably and may spread to different parts of the body. In 2020, the International Agency for Research on Cancer (IARC) estimated a total of 19.3 million new cancer cases and about 9.96 million deaths from cancer worldwide[1]. They further reported that by 2040, the number of new cancer cases is expected to rise to 30.2 million, with an estimated 16.3 million deaths from cancer worldwide. Additionally, it was reported that 70% of deaths from cancer occur in low-income and middle-income countries. This may be a result of the growing and aging population in these countries with poorer health care systems, and because preference is given to other diseases such as Human Immunodeficiency Virus/Acquired Immune Deficiency Syndrome (HIV/AIDS) in Africa. These statistics make it clear that there is a need for early detection, improve on current treatments and identify newer anti-cancer therapies to address this global concern.

1.2 Current anti-cancer treatments

Anti-cancer therapies are mainly designed to limit/stop the growth and spread of cancer cells. Currently, many different treatment methods are used to treat cancer including surgery, radiation therapy, chemotherapy, targeted therapy, immunotherapy and hormone therapy. Often, depending on the stage of cancer progression and the type of cancer, a combination of different therapies is used to maximise the therapeutic outcome. This reduces the possibility of drug resistance and also limits the toxicity of individual cancer drugs by treating patients with drugs that have different modes of action at the same time (1).

[1] Global cancer statistics as of 2020. Available from: https://gco.iarc.fr/today/data/factsheets/populations/900-world-fact-sheets.pdf

Conventional chemotherapy is one of the most common choices of cancer treatment which primarily functions by targeting rapidly proliferating cells. However, it is a non-specific process because cancer and non-cancer rapidly proliferating cells cannot be distinguished, thereby killing both (2). This leads to adverse side-effects in patients, such as nausea, myelosuppression and vomiting (3). Therefore, in order to reduce side-effects, there is a need to identify alternative treatments that are more specific and favourably target cancer cells over non-cancer cells. These types of newer therapies are called targeted therapies.

1.3 Targeted anti-cancer therapy

Targeted cancer therapy is the prevention of cancer growth and spread by precisely targeting specific molecules that are involved in cancer progression and are found to be dysregulated in cancer tissue compared to normal. Unlike conventional chemotherapy, targeted therapies are proposed to be more specific and preferentially target cancer cells, and anticipated to have lower toxicity in off-target cells (4). The main types of targeted therapy include small molecule inhibitors and monoclonal antibodies (mAbs). Small molecule inhibitors are low molecular weight compounds (<900 Daltons) that are able to enter cells and target specific intracellular proteins while monoclonal antibodies are larger compounds that target extracellular proteins to inhibit cancer progression (5).

Recent advances in genomic and proteomic techniques have allowed for the identification of cancer targets, where researchers sequence cancer DNA or protein and investigate gene expression patterns to identify genes or proteins that are dysregulated in cancer tissue compared to normal, in order to identify potential targets for anti-cancer therapies (5). After identifying a potential target, compounds are then identified or designed to inhibit these targets in the early stages of drug discovery. Small molecule inhibitors can be identified through *in silico* screening where the target molecule is screened against a library of test compounds computationally to identify inhibitor molecules that would best bind the target.

Our laboratory has an interest in recently identified novel cancer targets that include the nuclear transport proteins as members of this protein family has been shown to have dysregulated expression in cancer. Studies performed in our laboratory showed that specific nuclear transport proteins were significantly overexpressed in cervical cancer cells compared to normal, and were important for cell survival (6). Therefore, there is an interest in identifying small molecule inhibitors that target and inhibit members of the nuclear transport protein family that have altered expression in cancer as a potential targeted anti-cancer strategy.

1.4 Nuclear transport proteins

The nucleus is enclosed with a double phospholipidic membrane called the Nuclear Envelope (NE) to allow spatial separation between the nucleus and the cytoplasm, allowing regulation of processes that occur in each region separately (7). Therefore, specific proteins called nuclear transport proteins are required for the transport of cargo molecules between the nucleus and cytoplasm to allow for processes to take place simultaneously in different compartments of the cell.

Nuclear transport proteins are a group of soluble proteins that are involved in the transport of cargo molecules into or out of nucleus through the Nuclear Pore Complex (NPC). The NPC is a cylindrical channel made up of 30 different proteins called nucleoporins (Nups) with a molecular mass of approximately 125,000 kDa (8). There are between 2000 and 5000 NPCs present on average on a nuclear envelope within a vertebrate cell to allow for efficient nuclear transport (9). Cargo proteins travel through the NPC either by passive diffusion or facilitated diffusion, based on their size. Proteins smaller than 20-40kDa passively diffuse through the NPC while proteins larger than 40-65kDa pass through by facilitated diffusion with the aid of nuclear transport proteins (10). These proteins belong to a family of proteins called the Karyopherin family, which mediate the nuclear transport process.

1.5 Karyopherin proteins

The Karyopherin protein family is made up of a number of transport receptors which are responsible for shuttling cargo molecules into or out of the nucleus, depending on the nuclear or cytoplasmic demand. These cargo molecules include proteins, RNA, transcription factors, nuclear receptors and enzymes (11). This protein family is further divided into two subfamilies; the alpha (α) and beta (β) subfamily, where Karyopherin proteins that transport cargo molecules into the nucleus are called Importins while the proteins that transport cargo molecules out of the nucleus are called Exportins. The Importins and Exportins belong to the β subfamily and may either transport cargo molecules on their own *or* through the aid of adapter proteins from the α subfamily. The Karyopherin proteins identified to date are summarised in Table 1.1 below.

Table 1.1. Karyopherin β import (with α adapter proteins) and export proteins.

Karyopherin β Import proteins	**Karyopherin β Export proteins**	**Karyopherin β Import and export proteins**
Karyopherin beta 1 (KPNβ1) OR Importin β Transportin 1 (TNPO1) Transportin 2 (TNPO2) Importin 4 (IPO4) Importin 5 (IPO5) Importin 7 (IPO7) Importin 8 (IPO8) Importin 9 (IPO9) Importin 11 (IPO11) <u>α Adapter proteins:</u> Karyopherin alpha 1 (KPNα1) Karyopherin alpha 2 (KPNα2) Karyopherin alpha 3 (KPNα3) Karyopherin alpha 4 (KPNα4) Karyopherin alpha 5 (KPNα5) Karyopherin alpha 6 (KPNα6) Karyopherin alpha 7 (KPNα7)	Exportin 1 (XPO1) OR Chromosomal Region Maintenance 1 (CRM-1) Exportin 2 (XPO2) OR Chromosome segregation 1-like (CSE1L) OR Cellular Apoptosis Susceptibility (CAS) Exportin 5 (XPO5) Exportin 6 (XPO6) Exportin t (XPOT) Ran binding protein 17 (RANBP17)	Importin 13 (IPO13) Exportin 4 (XPO4) Exportin 7 (XPO7) Transportin 3 (TNPO3)

The nuclear transport process begins when Karyopherin proteins recognise a specific type of transport signal present on cargo proteins, either a Nuclear Localisation Signal (NLS) for nuclear import or a Nuclear Export Signal (NES) for nuclear export (12). Karyopherin proteins may transport cargo molecules either through the aid of adapter proteins in the classical pathway *or* on their own without binding to any other proteins in the non-classical pathway. During nuclear import in the classical pathway, a Karyopherin α adapter protein recognises and binds the NLS present on the cargo molecule and forms a dimer. A Karyopherin β protein then bind this dimer to form a trimeric complex that is now ready for transport into the

nucleus through the NPC. Once inside the nucleus, a protein called RanGTP binds to Karyopherin β with higher affinity than Karyopherin α leading to the dissociation of the trimeric complex and releasing the cargo molecules inside the nucleus. The RanGTP - Karyopherin β complex then transports back into the cytoplasm where RanGTP is converted to RanGDP, allowing Karyopherin β to be released in the cytoplasm for further rounds of nuclear import (13). During nuclear import in the non-classical pathway, the same order of events take place as the classical pathway, with the exception of it not requiring a Karyopherin α adapter protein aiding the transport process, as the Karyopherin β protein is able to transport the cargo molecules containing an NLS into the nucleus on its own. During nuclear export, a Karyopherin β exporter protein recognises and binds the NES present on cargo molecules, forming a dimer. RanGTP present inside the nucleus then binds to the dimer forming a complex that is ready for nuclear export. Once the complex has transported to the cytoplasm, RanGTP hydrolyses into RanGDP causing the dissociation of the cargo molecules in the cytoplasm (14) (Figure 1.1). Therefore, generally, binding of RanGTP to import proteins causes the release of cargo molecules in the nucleus while hydrolysis of RanGTP bound to export proteins causes the release of cargo molecules in the cytoplasm (12).

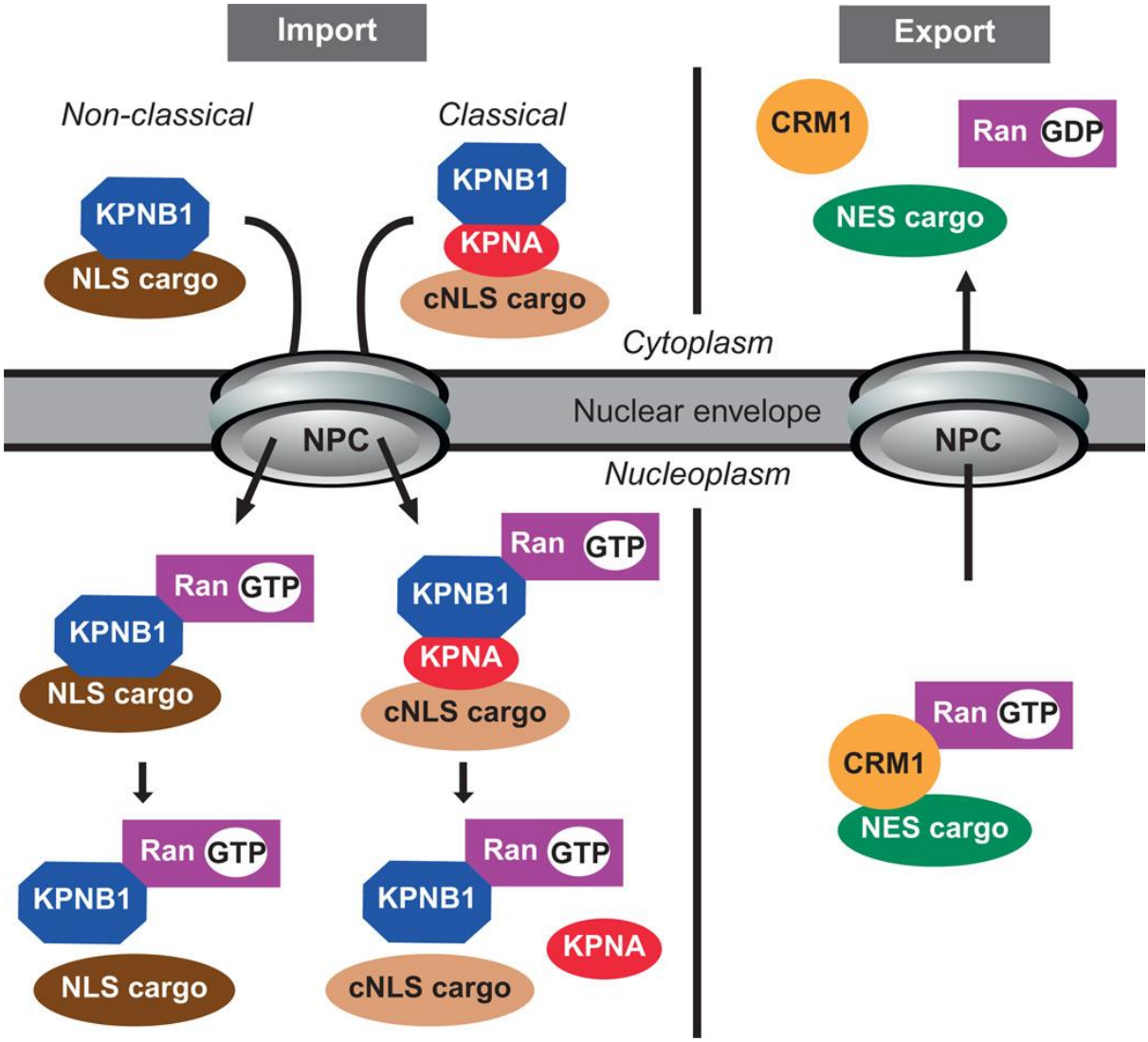

Figure 1.1. A representative image of the nuclear import and export pathways, facilitated by Karyopherin β proteins. KPNβ1 (importer protein) is used as an example to show the nuclear import pathway and CRM1 (exporter protein) is used as an example to demonstrate the nuclear export pathway. During nuclear import, in the non-classical pathway (left), KPNβ1 binds the cargo molecule containing an NLS and transports it into the nucleus through the NPC. Inside the nucleus, the KPNβ1-cargo complex binds to RanGTP causing dissociation of the cargo molecule inside the nucleus. In the classical pathway (middle), the adapter protein KPNα binds the cargo molecule containing an NLS and subsequently to KPNβ1 forming a trimeric complex which transports into the nucleus via the NPC. Once inside the nucleus, binding with RanGTP causes dissociation of the trimeric complex and release of the cargo molecule in the nucleus. During nuclear export (right), CRM1 binds to a cargo molecule containing an NES and further binds to RanGTP, forming a complex that transports out of the nucleus into the cytoplasm where breakdown of RanGTP causes dissociation of the cargo molecule in the cytoplasm. Image obtained from Hall et al., 2011 (15).

Although the main function of the Karyopherin proteins are for nuclear transport of cargo molecules, they have function in other cellular processes including mitosis and mitotic spindle assembly, in DNA replication in the S-phase, for the progression of the cell cycle and in NPC assembly (13,16,17). This highlights the importance of correct cellular functioning of the Karyopherin proteins because a change/disruption in function/expression may lead to serious consequences, including cancer. Research over the past few years have showed that expression of members of the Karyopherin protein family is dysregulated in cancer tissue compared to normal, making them potential diagnostic and therapeutic biomarkers.

1.6 Karyopherin proteins and cancer

Karyopherin proteins such as KPNβ1, CRM1, CSE1L and KPNα2 have been shown to be dysregulated in cancer cells compared to normal in different cancer types. A study by van der Watt et al. (2009) done in our laboratory reported that CRM1, KPNβ1 and KPNα2 are overexpressed in cervical cancer tissue (6). CRM1, also known as Exportin-1 is a well described nuclear export protein that transports cargoes including p53, Nuclear factor of activated T-cells (NFAT), Zinc finger protein SNAI1 (Snail) and Signal transducer and activator of transcription 3 (Stat3), amongst others (18,19). It is proposed that overexpression of CRM1 facilitates the nuclear export of tumour suppressor proteins into the cytoplasm, allowing for cancer progression (20).

KPNβ1, also known as Importin β, is a nuclear import protein that transports cargo molecules from the cytoplasm into the nucleus through the NPC, either through the aid of an adapter protein KPNα, or on its own (Figure 1.1). KPNβ1 imports cargoes such as transcription factors including NFAT, Nuclear factor kappa-light-chain-enhancer of activated B cells (NF-κB) and Snail, and proteins such as Stat3, Parathyroid Hormone-related Protein (PTHrP) and cyclin-B1, among others (21,22). It is suggested that the overexpression of KPNβ1 and KPNα2 in cervical cancer could be as a result of a dysregulation of the E2F and Rb complex in response to the Human Papillomavirus (HPV), which is responsible for majority of cervical cancer cases. The Retinoblastoma (Rb) protein is a tumour suppressor that binds to the transcription factor, E2F to negatively regulate the cell cycle and cell progression. In cervical cancer, the HPV

oncoprotein, E7 inhibits Rb leading to a dysregulation of E2F/Rb complex which is associated with the increased expression of KPNβ1 and KPNα2 (23).

Karyopherin proteins; KPNβ1, CRM1, CSE1L and KPNα2 have been reported to be overexpressed in other cancer types in studies looking at single cancer types. This is summarised in Table 1.2 below. Additionally, other Karyopherin proteins which are not included in Table 1.2 have also been reported to be overexpressed in cancer cells compared to normal. However, these have not been reported as extensively across multiple cancer types as the four Karyopherin's listed in Table 1.2. For example, KPNα7 was reported to be overexpressed in pancreatic cancer, XPO4 was reported to be overexpressed in liver cancer and XPO5 was reported to be overexpressed in colorectal cancer (24–26). It is suggested that elevated expression of Karyopherin proteins in cancer allows for increased nuclear transport rates, in order to maintain the higher metabolic and proliferative demand of cancer cells (6).

Table 1.2. A list of Karyopherin genes/proteins and the respective cancer types in which they are overexpressed.

Karyopherin β:	**Cancer type in which KPNβ1 is overexpressed:**
KPNβ1	Cervical (6), breast (27), ovarian (28), prostate (29), gastric (30), lung (31), colorectal (32), glioblastoma (33), chronic myeloid leukaemia (34), melanoma (35), bladder (36), hepatocellular carcinoma (37), head and neck (38), B-cell lymphoma (39).
CSE1L	Breast (40), hepatocellular carcinoma (41), gastric (42), ovarian (43), colorectal (44), lung (45), oral (46), bladder (47), non-Hodgkin's lymphoma (48), pancreatic (49), leukaemia (50).
CRM1	Cervical (6), oesophageal (51), ovarian (52), gastric (53), brain (54), head and neck (55), pancreatic (56), osteosarcoma (57), acute myeloid leukaemia (58).
KPNα2	Cervical (23), oesophageal (59), breast (60), gastric (61), ovarian (62), liver (63), lung (64), prostate (65), bladder (66), brain (54), melanoma (67), gallbladder (68), urothelial (69).

It is thus evident that Karyopherin protein dysregulation occurs in many cancer types. In our laboratory, we have an interest in KPNβ1 as a novel cancer biomarker and therapeutic target. We hypothesise that inhibiting KPNβ1 may be a potential targeted anti-cancer strategy for

cancers that overexpress KPNβ1 and inhibiting it may target cancer cells more specially in comparison to non-cancer cells.

1.7 KPNβ1 inhibition

In a study done in our laboratory, when KPNβ1 expression was inhibited using siRNA in cervical cancer cells, a significant reduction in cancer cell viability and proliferation was observed whilst non-cancer cells were relatively unaffected (70). This suggests that the inhibition of KPNβ1 with small molecules could have therapeutic potential. However, targeting KPNβ1 using drugs is still a very novel approach, therefore few anti-KPNβ1 drugs have been identified to date. Karyostatin A and Importazole were amongst the first small molecules identified to inhibit KPNβ1 (71,72). Both are proposed to interfere with the binding of RanGTP to KPNβ1 thereby inhibiting transport of cargo molecules into the nucleus. Both of these inhibitors have shown anti-cancer potential in cell culture models thus far, but neither have been tested in clinical trials as of yet (70). Another inhibitor targeting KPNα is the FDA-approved antiparasitic agent, Ivermectin. Ivermectin is capable of inhibiting the replication of viruses such as HIV-1 and dengue virus but has also shown anti-cancer potential in some studies. For example, it has shown potential in decreasing tumour formation *in vivo* and *in vitro* during hepatocarcinogenesis (73,74). In our laboratory, a novel small molecule inhibitor of KPNβ1 was identified named Inhibitor of Nuclear Import-43, INI-43 (chemically known as 3-(1H-benzimidazol-2-yl)-1-(3-dimethylaminopropyl)pyrrolo[5,4-b]quinoxalin-2-amine) (Figure 1.2). This molecule has been studied extensively in our laboratory for its effects on cervical cancer cells using both *in vitro* and *in vivo* assays. INI-43 has shown promise as a potential inhibitor of KPNβ1 associated nuclear import pathways that associate with the killing of cervical cancer cells.

1.8 Identification of INI-43 and inhibition of KPNβ1 nuclear import

INI-43 is a chemical compound that was identified through *in silico* screening in collaboration with the Molecular Modelling Facility of the James Graham Brown Centre at the University of Louisville, Kentucky, USA. A structure-based computational screen was performed using the

known crystal structure of KPNβ1 to identify small molecules that bind to KPNβ1 in the overlapping Ran and KPNα2 binding sites of KPNβ1 (using PDB codes 1ibr, 2bku, and 1qgk), as these are sites that are essential for the nuclear import process. A library of compounds was screened, and compounds were ranked according to their binding affinity to KPNβ1, of which forty-seven of the highest ranked compounds were selected and tested in cell culture models to determine if inhibitory effects was observed on cancer cell viability and KPNβ1 associated nuclear import function. INI-43 was amongst the top ranked compounds tested that showed a significant cell killing effect and inhibition of KPNβ1 activity. Compounds were also screened for their effects on nuclear import, whereby the nuclear translocation of a KPNβ1 cargo, NFAT was assayed. Cells were transfected with an NFAT expression construct and NFAT-luciferase construct, and effects of the compounds on NFAT nuclear import were determined using a luciferase assay, after its induction using PMA/Ionomycin. INI-43 was highly effective at inhibiting NFAT nuclear translocation, revealing its effectiveness in blocking nuclear import pathways (70).

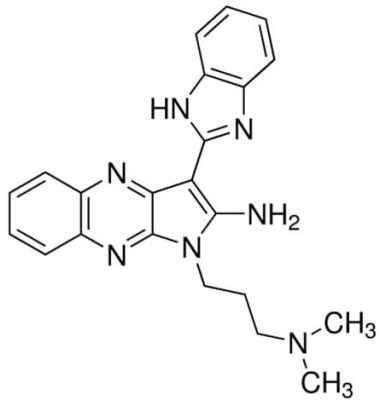

Figure 1.2. Chemical structure of INI-43 (3-(1H-benzimidazol-2-yl)-1-(3-dimethylaminopropyl)pyrrolo[5,4-b]quinoxaline-2-amine).

Further investigation revealed that INI-43 resulted in cytotoxic effects in cervical cancer cells at a concentration of approximately 10 μmol/L. An inhibition of cervical cancer cell proliferation was also observed, followed by G2-M cell cycle arrest and cancer cell death by apoptosis. The effects of INI-43 on cervical cancer cell lines, were in line with that observed using siRNA against KPNβ1. Cancer cell death effects induced by INI-43 were rescued by KPNβ1 overexpression providing evidence that the small molecule acts on KPNβ1. Additionally, it was determined that INI-43 is able to inhibit the nuclear import of various

KPNβ1 cargoes, including AP-1 and NFkB. Further studies showed that INI-43 also decreased tumour growth in *in vivo* xenograft mouse models, of both cervical cancer and oesophageal cancer origin (70). This shows that INI-43 is a promising candidate for targeted anti-cancer therapy. Considering that KPNβ1 has elevated expression in many cancer types, it is of interest to investigate if INI-43 has inhibitory effects on cancer types of different tissue origins. In addition, it is of interest to determine if INI-43 exerts its effects by primarily binding to KPNβ1 as hypothesised.

1.9 Importance of precise drug binding

A drug needs to bind to its cognate target to ensure its desired therapeutic outcome, and the binding of a drug to off-target proteins can have negative consequences. When a drug interacts with the target, it either activates or deactivates it, leading to the desired cellular, molecular and physiological effects. However, non-specific binding of the drug to an off-target protein may lead to toxicity and unwanted side-effects (75). For example, Iniparib is an anti-cancer drug that was thought to function as a poly(ADP–ribose) polymerase (PARP) inhibitor after showing inhibitory effects in breast cancer cells. It was then tested in clinical trials where after initial success in preclinical trials, Phase I and Phase II clinical trials, Iniparib failed in Phase III clinical trial due to a lack of efficacy in patients. Thereafter, target engagement studies conducted showed that Iniparib did not bind to PARP but instead the likely cause of the initial anti-proliferative effects observed were probably due to Iniparib generating reactive oxygen species intracellularly (76). This highlights the importance of a drug binding to its correct hypothesised target. In this project, we therefore, aim to determine if INI-43 exhibits inhibitory effects by binding to KPNβ1.

Different biophysical assays have been established over the years to monitor drug:target engagement in cells. This includes methods that use resonance energy transfer such as Fluorescence Resonance Energy Transfer (FRET) and Bioluminescence Resonance Energy Transfer (BRET), other methods include Affinity-Based Chemical Proteomics, Ligand-Directed Protein Labeling and Enzyme Fragment Complementation Assay (77). Previous work in our laboratory used the biophysical assays GST biosensors and Super Streptavidin (SSA)

biosensors (Aderonke Fopesaye Ajayi-Smith, PhD thesis, 2019) and Circular Dichroism and Isothermal Titration Calorimetry (Erin Strydom, PhD thesis, 2016) to study drug:protein interaction. These studies showed that INI-43 interacts with purified KPNβ1. While these biophysical assays are gold standard, they require purified proteins and therefore, do not show drug:protein interactions inside living cells. For that reason, in this project, we aim to determine if INI-43 binds to KPNβ1 using the biophysical assay, Cellular Thermal Shift Assay (CETSA) which is a modification-free approach that studies drug:protein interaction inside living cells.

1.10 Significance

Studies in our laboratory have reported that KPNβ1 is overexpressed in cervical cancer cells and treatment with INI-43 showed cytotoxic effects and inhibited KPNβ1-associated nuclear import pathways in these cancer cells. While expression of KPNβ1 has been reported in some cancer types, little is known on the effect of INI-43 on cancers of different tissue origins. This study aims to broaden our knowledge on KPNβ1 expression and the potential for application of INI-43 as an anti-cancer therapeutic in multiple cancer types.

Furthermore, since a direct interaction between KPNβ1 and INI-43 has not been determined experimentally in living cells, this study will investigate if there is an interaction between KPNβ1 and INI-43. This may assist in ruling out potential cytotoxic effects that may be due to off-target engagements. This is important knowledge if INI-43 is to be considered further in the drug development pipeline.

1.11 Project aims

This project aims:

1. To determine KPNβ1 mRNA levels in cancer patient samples of varied tissue origin in comparison to non-cancer using bioinformatic approaches.

2. To determine KPNβ1 protein expression in cancer cell lines of different tissue origin.

3. To investigate the 50% Cytotoxic Concentrations (CC_{50}) of INI-43 on cancer and non-cancer cell lines representative of cancers of varied tissue origin.

4. To investigate drug:protein interactions inside cells to determine if INI-43 directly binds to KPNβ1.

Chapter 2

Materials and Methods

2.1 Materials

2.1.1 Cell lines

The following cell lines are from the American Type Culture Collection (ATCC) (Rockville, MD, USA): human cervical carcinoma cell lines, HeLa, SiHa and ME180; breast carcinoma cell lines, MDA-MB231, MCF7 and T47D; fibrosarcoma cell line, HT1080; gastric carcinoma cell line, KatoIII; human immortalised retinal epithelial cell line, hTERT RPE-1 and human primary retinal epithelial cell line, ARPE-19. The human oesophageal squamous carcinoma cell line, WHCO5 was originally established from a South African patient with oesophageal squamous cell carcinoma and acquired from Professor R. Veale from the University of Witwatersrand while the human oesophageal squamous carcinoma cell line, KYSE30 was obtained from DSMZ (Berlin, Germany). The human osteosarcoma cell line, U2OS and human transformed cervical epithelial cells, End1/E6E7 were kindly gifted by Professor J. Hapgood at the University of Cape Town. The human liver cancer cell line, HepaRG was kindly provided by Dr Hlumani Ndlovu at the University of Cape Town and purchased from Lonza. The normal human immortalised oesophageal keratinocytes, EPC2 were kindly gifted by Prof. A. K. Rustgi from the University of Pennsylvania.

2.1.2 Chemical compounds

Inhibitor of Nuclear Import-43, INI-43 (chemical name 3-(1H-benzimidazol-2-yl)-1-(3-dimethylaminopropyl)pyrrolo[5,4-b]quinoxalin-2-amine) was obtained in powder form from Sigma-Aldrich (CAS number 881046-01-1). The compound was dissolved in DMSO to a stock concentration of 10 mM and stored at room temperature. The drug is light-sensitive, therefore it was wrapped in foil and protected from light when stored.

2.2 Methods

2.2.1 Bioinformatic analyses

2.2.1.1 *In silico* analyses of KPNβ1 gene expression in patients

To investigate mRNA expression of KPNβ1 in cancer tissue compared to corresponding normal tissue, various online open access databases were used, including Oncomine (78), The Cancer Genome Atlas (TCGA) and The Genotype-Tissue Expression (GTEx) project.

2.2.1.2 Survival plots

To investigate the correlation between KPNβ1 expression and patient prognosis, Kaplan Meier plots showing overall survival (OS) were obtained for various cancer types using the Kaplan-Meier (KM) Plotter (https://kmplot.com/), which analyses data from the Gene Expression Omnibus (GEO), European Genome-Phenome Archive (EGA) and TCGA. Patient groups were separated using the best cut-off feature. Cancer types where n>200 patients were selected.

2.2.2 Cell culture

All cell lines, except KatoIII, EPC2, End1, hTERT-RPE1 and ARPE-19 were cultured in Dulbecco's Modified Eagle's Medium (DMEM) (Invitrogen, USA) supplemented with penicillin (100 U/ml), streptomycin (100 µg/ml) and 10% Fetal Calf Serum (FCS) (Gibco, Paisley, Scotland). KatoIII, an adherent and suspension cell line, was maintained in Iscove's Modified Dulbecco's Medium (IMDM) (Gibco) supplemented with penicillin (100 U/ml), streptomycin (100µg/ml) and 20% FCS (Gibco). EPC2 and End1 cell lines were cultured in Keratinocyte Serum Free Medium (KSFM) (Gibco) supplemented with 1 ng/ml epidermal growth factor (EGF), 50 µg/ml bovine pituitary extract (BPE), penicillin (100 U/ml) and streptomycin (100 µg/ml). End1 cells were further supplemented with 0.4 mM calcium chloride. ARPE-19 and hTERT-RPE1 were maintained in DMEM:F12 media (Gibco), supplemented with penicillin (100 U/ml), streptomycin (100µg/ml) and 10% FCS (Gibco). hTERT-RPE1 cells were further supplemented

with 0.01 mg/mL of Hygromycin B (Sigma-Aldrich). All cells were cultured in 100mm tissue culture dishes and grown in a humidified incubator at 95% air and 5% CO_2 at 37°C.

2.2.3 Protein harvest

Cells in culture were grown to 80% confluency in 60 mm tissue culture dishes. Cells were washed with ice cold 1 X PBS and harvested in complete RIPA buffer (see Appendix I - Solutions) containing 1 X complete protease inhibitor cocktail (Roche, Basil, Switzerland) and 0.1 M Sodium Orthovanadate (Na_3VO_4) phosphatase inhibitor. Cells were scraped using a cell scraper and collected into sterile eppendorf tubes. Cell lysates were then sonicated for 8-10 seconds and centrifuged at 10000 rpm at 4°C for 10 minutes using the Biocen 22 R microcentrifuge (Orto Alresa, United Scientific) to pellet cellular debris. The supernatant containing the cellular protein was then collected into new sterile eppendorf tubes and stored at -80°C until protein quantification and Western blotting.

2.2.4 Protein quantification

Protein concentrations were determined using a Bicinchoninic Acid (BCA) protein assay kit (Pierce, ThermoScientific, USA), according to the manufacturer's instructions. This assay is based on the colour change from green to purple due to the reduction of Cu^{2+} to Cu^{1+} under alkaline conditions (Biuret reaction). The colour change is measured using a spectrophotometer at an absorbance of 595nm and is representative of the total protein present in a sample. A Bovine Serum Albumin (BSA) standard curve was constructed using concentrations ranging from 100 µg/ml to 2000 µg/ml of BSA. 100 µl of the BCA working solution was added to 10 µl of each protein and BSA concentration in duplicate in a 96-well plate. This was incubated at 37˚C for 30 minutes and absorbance values were read at 595nm using a BioTek microplate spectrophotometer. Using the BSA standard curve, the protein concentration for each sample was determined.

2.2.5 Western blot analysis

SDS polyacrylamide gels were prepared, using a 10% resolving/separating gel and 4% stacking gel on top. A fixed concentration of protein (30 µg) from each cell line was combined with 4X loading dye and made up to 25 µl with RIPA buffer, and subsequently heated at 90˚C for 5 minutes in a heating block to denature the proteins. The mixtures were then loaded into the wells of the stacking gel, alongside 5 µl of a protein ladder (Colour Protein Standard, BioLabs, New England) which was used as a size reference for the proteins. The gels were then electrophoresed at 180V for one hour in 1 X Running Buffer (see Appendix I - Solutions) and protein was transferred to Hybond™-ECL™ nitrocellulose membranes (Amersham Biosciences, Buckinghamshire, UK) using ice cold 1 X Transfer Buffer (see Appendix I - Solutions) at 100V for 70 minutes. Thereafter, membranes were blocked in 5% milk in TBST for one hour with gentle shaking to prevent any non-specific binding. The membranes were then incubated with primary antibody at 4˚C overnight. The following day, the membranes were washed three times for 5 minutes each with 1 X TBST. The membranes were then probed with secondary antibody conjugated with horseradish peroxidase (HRP) for one hour with gentle shaking and then washed again three times with 1 X TBST for 5 minutes. The antibody conditions used are summarised in Table 2.1 below. The protein bands were then detected using the chemiluminescent substrate LumiGlo (KPL, SeraCare Life Sciences, Milford, USA) and visualised using the iBright™ 1500 Imaging System (ThermoScientific, USA). Western blot bands were quantified using ImageJ software version 1.53t.

Table 2.1. Primary and secondary antibody conditions used.

Primary Antibody	Primary Antibody conditions	Secondary Antibody	Secondary Antibody conditions
KPNβ1 [ab45938, Abcam]	1:5000 TBST	Goat-anti-rabbit [Bio-Rad]	1:5000 in TBST
KPNα2 [#14372, Cell Signalling]	1:1000 5% milk in TBST	Goat-anti-rabbit [Bio-Rad]	1:5000 in TBST
CAS [SAB1400055, Sigma-Aldrich]	1:1000 TBST	Goat-anti-mouse [Bio-Rad]	1:5000 in TBST
CRM1 [sc-5595, Santa Cruz Biotechnology]	1:1000 TBST	Goat-anti-rabbit [Bio-Rad]	1:5000 in TBST
TNPO1 [TO825, Sigma-Aldrich]	1:1000 TBST	Goat-anti-mouse [Bio-Rad]	1:5000 in TBST
IPO5 [SAB4200179, Sigma-Aldrich]	1:1000 5% milk in TBST	Goat-anti-rabbit [Bio-Rad]	1:5000 in TBST
GAPDH [G9545, Sigma-Aldrich]	1:10000 5% milk in TBST	Goat-anti-rabbit [Bio-Rad]	1:5000 in TBST

2.2.6 Re-probing of membrane

To strip membranes and re-probe with different antibody, membranes were washed with 1M Glycine, pH 2.5 on either side for 6 minutes each. To neutralise the blots, 1M Tris-Cl pH 7.5 was then added. Membranes were then washed three times with 1 X TBST for 5 minutes each and blocked in 5% milk in TBST for 30 minutes. Membranes were then probed with primary and secondary antibodies as previously described (Section 2.2.5).

2.2.7 CC_{50} determination

To determine the drug concentration that inhibits 50 % cytotoxicity concentration (CC_{50}), the MTT assay was used. Cells were plated at approximately 70 % confluency in 96-well plates and left to incubate for 24 hours. The next day, all cells were treated with varying concentrations of INI-43: 0, 1, 5, 7.5, 10, 15, 20 and 50 µM for 48 hours. After 48 hours, MTT (3-(4,5-dimethylthiazol-2-yl)-2,5-diphenyltetrazolium bromide) reagent (Sigma) was added for 4 hours, after which Solubilisation Reagent (10% SLS in 0.01 M HCl) was added to quantify the number of viable cells. Following an overnight incubation, absorbance was read at 595nm using a BioTek microplate spectrophotometer. Dose-response curves were generated using GraphPad Prism software and CC_{50} values were determined.

2.2.8 Apoptosis assays

To determine if cell death was taking place by apoptosis, the Caspase-Glo™ 3/7 Assay (Promega) was performed on ME180, HepaRG, MDA-MB231 and Kyse30 cell lines after treatment with INI-43, according to the manufacturer's instructions. Cells were plated in 96-well plates and treated with INI-43 for 24 hours. Caspase-3/7 activity was then assayed using the Caspase-Glo 3/7 kit, and luminescence was monitored using the Glomax 96 Microplate Luminometer (Promega). Cells were standardised relative to an MTT assay that was set up simultaneously alongside the Caspase-Glo™ 3/7 Assay.

2.2.9 Fluorescence quantification

To determine the timepoint at which INI-43 is taken up into cells, HeLa cells were grown in 60 mm tissue culture dishes for 24 hours. The cells were then treated with 10 µM of INI-43 for up to 5 hours and images were captured using the Thermofisher EVOS M5000 fluorescent microscope at different timepoints. The fluorescent signal was quantified from fifty different cells at each timepoint using ImageJ and expressed as corrected total cell fluorescence (CTCF) to account for any background fluorescence given off in the samples where CTCF = Integrated Density – (Area of selected cell X Mean fluorescence of background readings).

2.2.10 Cellular Thermal Shift Assay (CETSA)

To investigate if INI-43 exerts its effects by directly targeting KPNβ1, Cellular Thermal Shift Assays were conducted using HeLa, ME-180 and SiHa cell lines. This is a technique that is used to validate drug binding based on changes in the thermal stability of proteins upon heating. In this experiment, cells from each cell line were cultured in duplicate in two separate 60mm tissue culture dishes and incubated for 24 hours until cells were 70-80% confluent. One dish of cells was used as the treated group (with INI-43) while the other dish served as the control (without INI-43). Intact cells were treated with 10 µM of INI-43 (treated group) while an equal volume of DMSO was added to the control intact cells and incubated at 37°C for 3 hours. Protein was then harvested from both treated and control cells using lysis buffer (see Appendix I - Solutions) containing 1 X complete protease inhibitor cocktail (Roche, Basil, Switzerland) and 0.1M Sodium Orthovanadate (Na_3VO_4) phosphatase inhibitor, and centrifuged at 14000xg for 20 minutes at 4°C using the Biocen 22 R microcentrifuge (Orto Alresa, United Scientific). Thereafter, supernatants from the treated and control samples were evenly divided into 8 aliquots, carefully, so as not to disturb the pellet. Each aliquot was then heated to a different temperature; 25°C, 45°C, 65°C, 70°C, 75°C, 77.5°C, 80°C and 82.5°C for 15 minutes. The aliquots were then centrifuged at 14000xg for 40 minutes at 4°C using the Biocen 22 R microcentrifuge (Orto Alresa, United Scientific) to obtain the soluble protein fraction. Supernatants were transferred to new eppendorf tubes and stored at -80°C until Western Blotting was carried out. KPNβ1 levels at each temperature for treated and corresponding controls were then determined through gel electrophoresis and Western blot analysis as described above (Section 2.2.5). Finally, protein bands were quantified using ImageJ and melt curves were generated using GraphPad Prism, using GAPDH as the loading control.

To investigate if INI-43 has off-target effects, CETSA experiments were also conducted to analyse the effects of INI-43 on other members of the Karyopherin protein family including KPNα2, Cas, CRM1, TNPO1 and IPO5, as well as GAPDH as a negative control. These experiments were conducted using the HeLa cell line.

2.2.11 Statistical analysis

Experiments were performed in triplicate and presented as mean ± standard error of mean (SEM), unless stated otherwise. All experiments were performed at least two independent times. For all data comparisons, the Student's t test was performed using Microsoft Excel and a p value of < 0.05 was considered statistically significant (indicated by *).

Chapter 3

Investigating the expression of KPNβ1 and the effect of INI-43 on different cancer types

3.1 Introduction

Research into targeted anti-cancer therapeutic drugs is becoming increasingly widespread because targeted therapies are anticipated to aid in reducing some of the side effects in patients that have been observed with conventional chemotherapeutic drugs. This is because targeted therapies function by specifically targeting only key proteins or pathways involved in driving tumorigenesis (4). One such protein of focus in our research group is the nuclear import protein, KPNβ1.

Previously published research in our laboratory and other studies have shown altered expression of KPNβ1 in cancer cells compared to non-cancer cells, suggesting that KPNβ1 plays a vital role in cancer cell biology. The elevated expression of KPNβ1 in cancer cells results in greater nuclear import of cargo molecules which is suggested to maintain the higher metabolic and proliferative demand of cancer cells (6). A pan-cancer study on KPNβ1 expression has not been conducted to date, however, smaller scale studies on a range of transformed cells have been analysed previously and showed the overexpression of KPNβ1 in transformed cells compared to the non-transformed counterparts (79). Furthermore, research in our laboratory has shown that inhibition of KPNβ1 using the small molecule inhibitor, INI-43 resulted in cervical cancer cell death by apoptosis and reduced cervical cancer cell proliferation (70). This suggests a dependency of cervical cancer cells on KPNβ1 for multiple biological processes required for their survival and proliferation. While studies in our laboratory have investigated the expression of KPNβ1 and inhibition of KPNβ1 in cervical cancer cells, a pan-cancer study is yet to be carried out to investigate the expression of KPNβ1 and the inhibitory effect of INI-43 in cancer types of different tissue origins.

The aim of this chapter is to investigate the expression of KPNβ1 and the effect of INI-43 on a panel of cell lines of different tissue origins that were available to us. To investigate the

expression of KPNβ1 at the genomic (mRNA) and proteomic level, we used bioinformatic approaches and Western blots, respectively. Bioinformatic approaches have become a useful tool in uncovering a vast amount of biological information that is made available to us from researchers globally. In this study, we used the bioinformatic databases, Oncomine, TCGA and GTEx project to retrieve information on the expression of KPNβ1 mRNA in patient tissues of different origin. To determine whether KPNβ1 expression had any correlation with patient survival, we used the online Kaplan Meier plotter (KM Plotter). In addition, KPNβ1 expression levels were monitored in a panel of cancer cell lines of different tissue origin that were available to us in the laboratory. To investigate the effect of INI-43 on cancer cell viability, the 50% cytotoxic concentration (CC_{50}) was measured after treatment of different cancer cell lines with INI-43. The CC_{50} is the concentration of a drug that is required to reduce cell viability by 50% after a specific exposure time (80). CC_{50} is a very useful measure to investigate the potency of a drug, where the lower the CC_{50} value, the lower the concentration of a drug is required to produce half the cytotoxic effect. An ideal CC_{50} value is one that is lower in the cancer cells compared to the CC_{50} value for the non-cancer cells.

Our results in this chapter show that there is altered expression of KPNβ1 in multiple cancer types, and that INI-43 has a greater cytotoxic effect on cancer cells compared to non-cancer cells, which supports that KPNβ1 has potential as a therapeutic target for multiple cancer types.

3.2 Results

3.2.1 KPNβ1 gene expression in cancer patient tissue compared to non-cancer tissue

To investigate whether KPNβ1 mRNA is differentially expressed between cancer patient tissue and non-cancer tissue, bioinformatic analyses were conducted using publicly available databases.

Firstly, Oncomine datamining was performed. Oncomine is a cancer microarray database which is used in the aid of genome-wide expression analyses and in uncovering any associations between gene expression and cancer. This is an open access database where data from different patient studies is deposited for researchers to retrieve and study. An Oncomine search was conducted to compare KPNβ1 levels in various cancer tissue types compared to non-cancer control tissues. The results revealed that 17 cancer types (including 44 cancer subtypes) of the 26 cancer types showed upregulated KPNβ1 mRNA expression in cancer tissue compared to non-cancer (using a cut-off of 1.5 fold upregulation and a p-value of <0.05). This included both solid and blood tumours. There were 29 different studies available that represented 17 of the cancer types that showed upregulation of KPNβ1. Additionally, 9 cancer types did not show any overexpression of KPNβ1. Figure 3.1 summarises the 44 cancer subtypes that showed upregulation of KPNβ1 mRNA expression, where bars highlighted in red are the cancer subtypes for which cell lines were available in our laboratory and included in subsequent investigation.

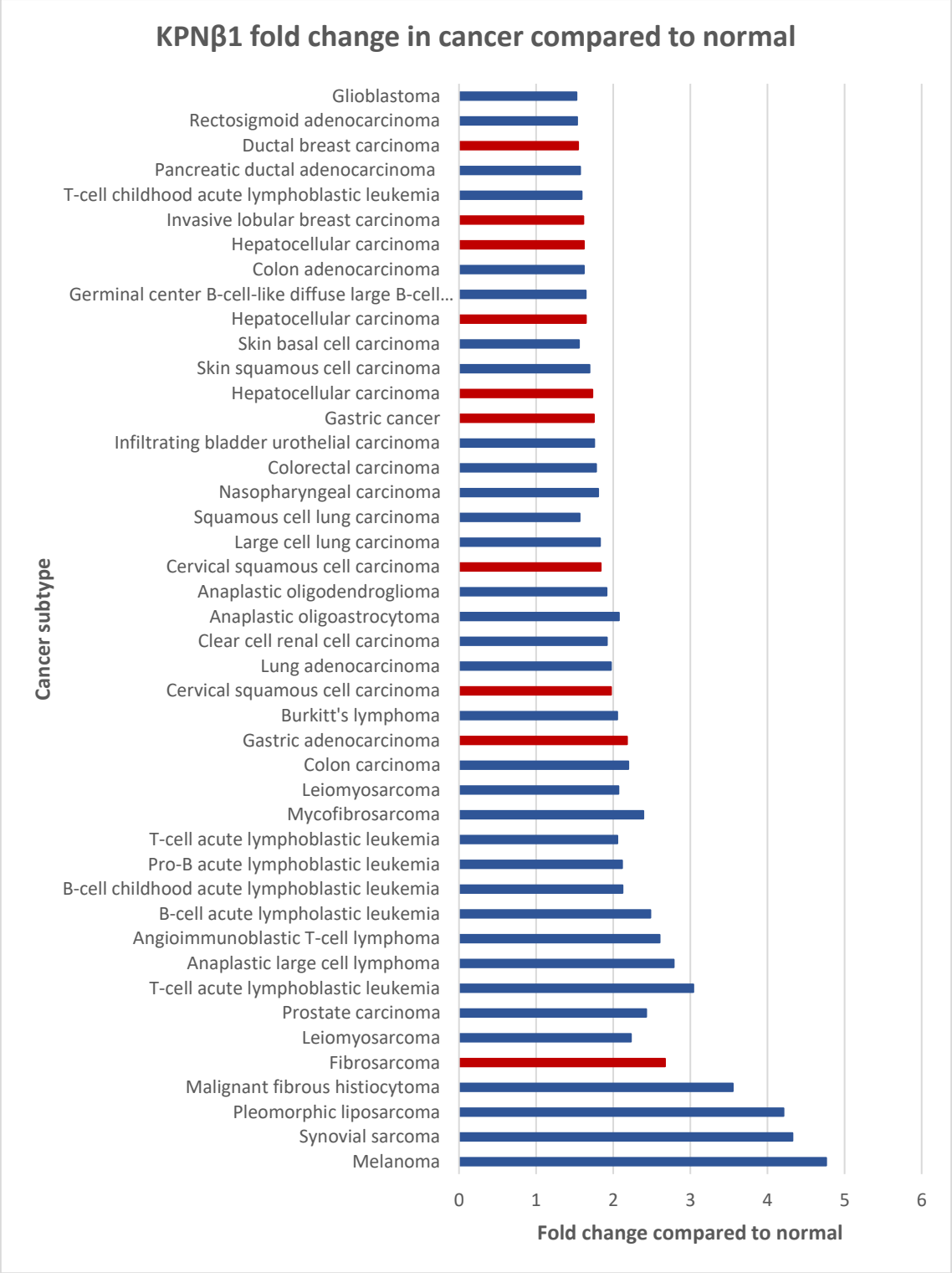

Figure 3.1. KPNβ1 gene expression is upregulated in various cancer tissues compared to their respective non-cancer tissues. Bar graph denoting the fold change of KPNβ1 gene expression in cancer tissue compared to non-cancer tissue, as obtained from patient data in the Oncomine microarray database. The data utilised was deposited into the database from different studies, hence some cancers are listed more than once. A cut-off of 1.5 fold upregulation was used to classify cancers that showed upregulation. Red bars indicate cancer subtypes for which cell lines were available in our laboratory and included in this study.

KPNβ1 mRNA levels were further examined using data obtained from The Cancer Genome Atlas (TCGA) and the Genotype Tissue Expression (GTEx) project. TCGA and GTEx are databases that compile large amounts of mRNA sequencing data from cancer and non-cancer patients, respectively. However, comparison of the data from the different databases is difficult. Therefore, Wang et al. (2018) unified the data by removing study specific biases using cancer data from TCGA and corresponding non-cancer data from GTEx, into one repository called Figshare (https://figshare.com/articles/dataset/Data_record_3/5330593), to allow direct comparison between the different datasets (81). KPNβ1 expression data was retrieved for 12 different cancer types, including 16 cancer subtypes, of which 12 of the 16 cancer subtypes showed significant upregulation of KPNβ1 mRNA expression in cancer compared to non-cancer (Figure 3.2), while 3 cancer subtypes showed no significant change (Figure 3.3 A). Interestingly, one cancer subtype; kidney chromophobe showed significant downregulation of KPNβ1 mRNA expression in cancer compared to non-cancer (Figure 3.3 B). Overall, 75% of cancer subtypes for which data was available showed a significant upregulation of KPNβ1 gene expression in cancer patients compared to non-cancer (Figure 3.4), highlighting that even though cancers may be different and are heterogenous within the same cancer type, they share some common patterns which can be targeted and utilised in anti-cancer therapy.

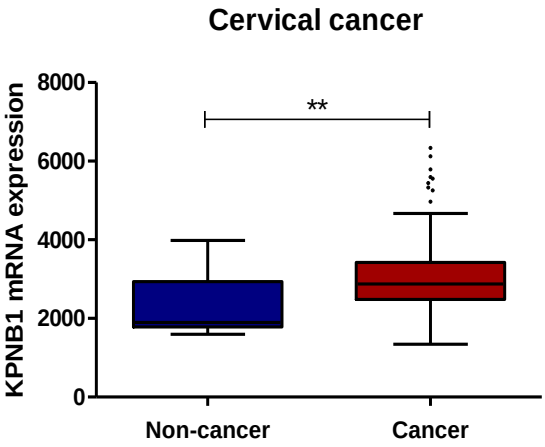
Cervical cancer
KPNB1 mRNA expression
8000
6000
4000
2000
0
**
Non-cancer
Cancer

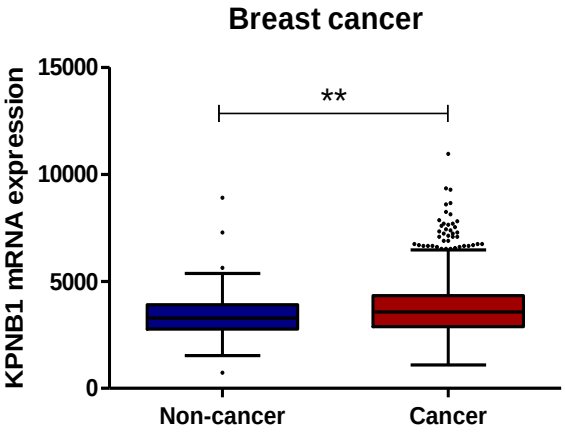
Breast cancer
KPNB1 mRNA expression
15000
10000
5000
0
**
Non-cancer
Cancer

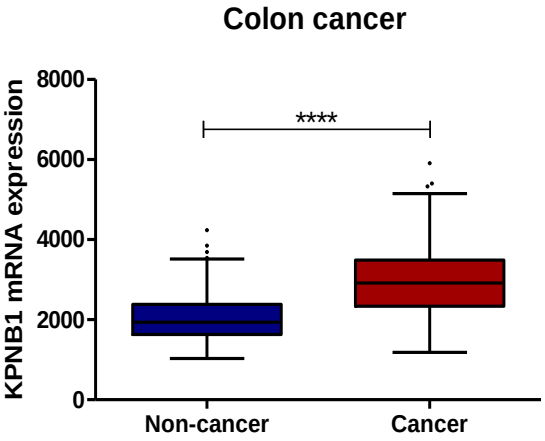
Colon cancer
KPNB1 mRNA expression
8000
6000
4000
2000
0
****
Non-cancer
Cancer

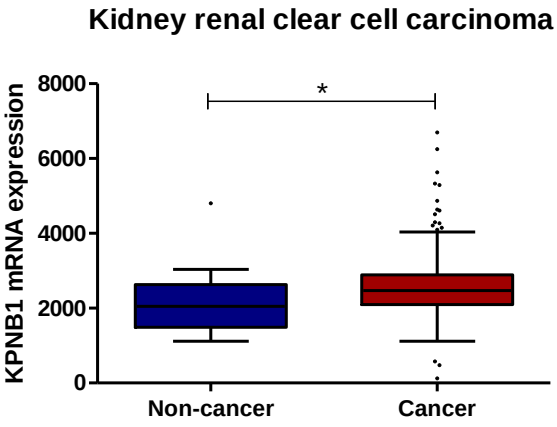
Kidney renal clear cell carcinoma
KPNB1 mRNA expression
8000
6000
4000
2000
0
*
Non-cancer
Cancer

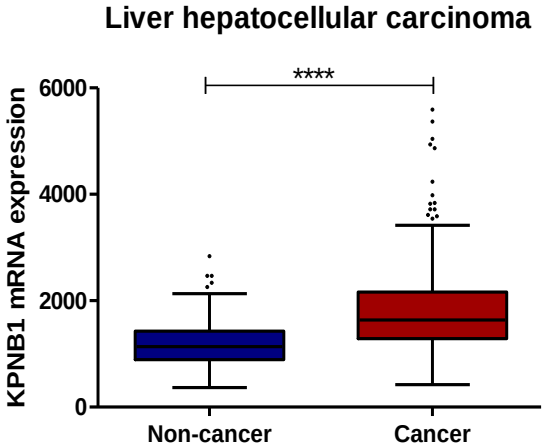
Liver hepatocellular carcinoma
KPNB1 mRNA expression
6000
4000
2000
0
****
Non-cancer
Cancer

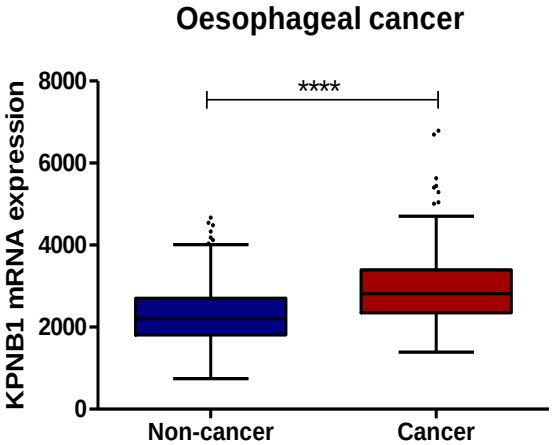
Oesophageal cancer
KPNB1 mRNA expression
8000
6000
4000
2000
0
****
Non-cancer
Cancer

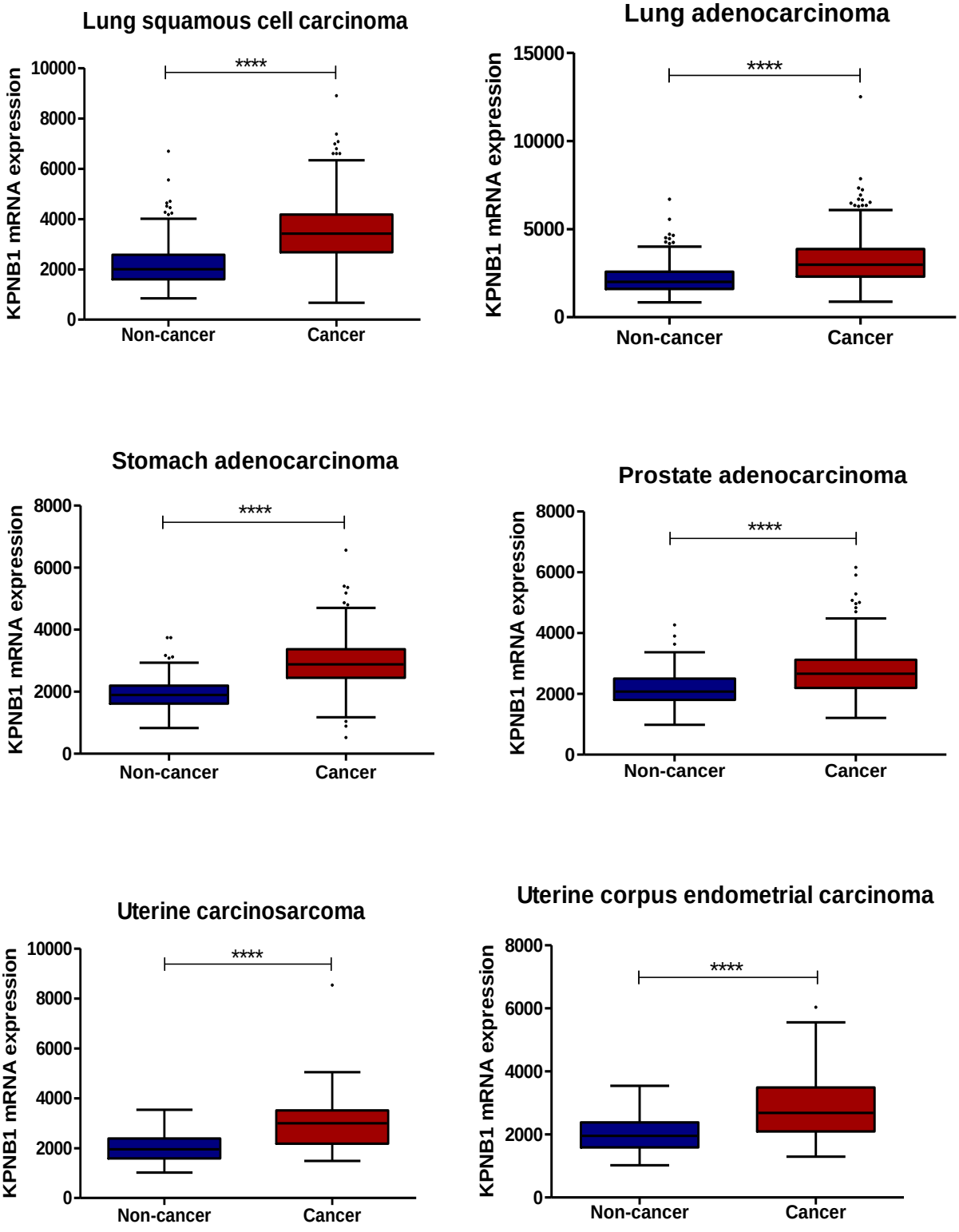

Figure 3.2. KPNβ1 gene expression in cancer patient tissue with elevated levels in comparison to respective non-cancer tissue. A TCGA-GTEx comparison was conducted on patient tissue and box and whisker graphs plotted, showing cancer subtypes where KPNβ1 was overexpressed in cancer tissue compared to respective non-cancer tissue (*p<0.05, **p<0.01, ****p<0.0001). Box and whisker plots were compiled using GraphPad Prism software.

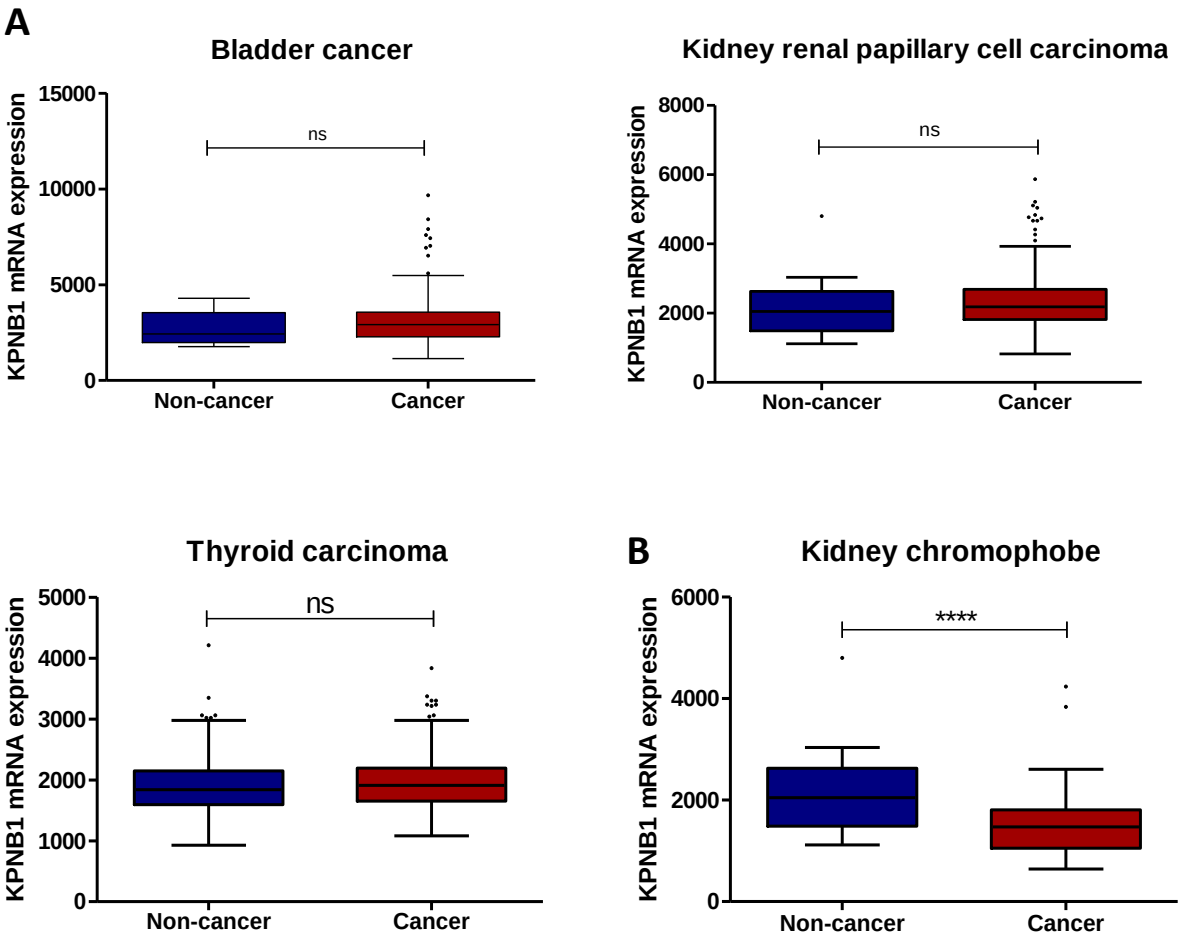

Figure 3.3. KPNβ1 gene expression in cancer patient tissue showing no change or decreased levels in comparison to respective non-cancer tissue. A TCGA-GTEx comparison was conducted on patient tissue and box and whisker graphs plotted, showing cancer subtypes where KPNβ1 was (A) not significantly different (ns>0.05) and (B) underexpressed in cancer tissue compared to respective non-cancer tissue (*p<0.05, ****p<0.0001). Box and whisker plots were compiled using GraphPad Prism software.

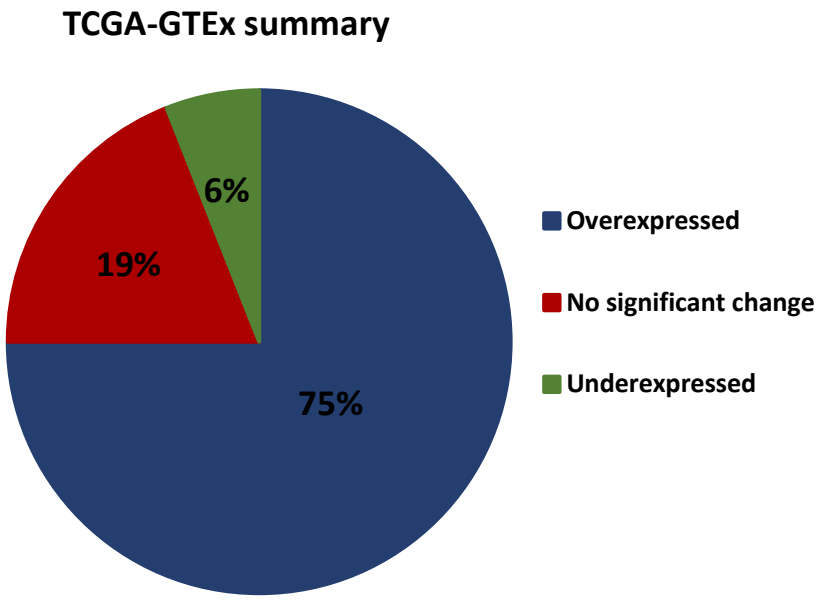

Figure 3.4. Pie chart showing the percentage of cancer types where overexpression, no significant change and underexpression of KPNβ1 was observed using a TCGA-GTEx comparison.

These results using publicly available data sources is in line with findings we have determined previously for cervical cancer in our laboratory, highlighting that KPNβ1 indeed appears to be elevated in multiple cancer types, suggesting that KPNβ1 could be a useful anti-cancer therapeutic target for various cancer types.

3.2.2 Determining a correlation between KPNβ1 gene expression and patient survival

Since KPNβ1 was found to be overexpressed in various cancer types, we next investigated if any correlation existed between KPNβ1 gene expression and patient survival. To this end, Kaplan Meier plots were drawn, showing overall survival (OS) relative to KPNβ1 expression, across multiple cancer patient groups using the Kaplan-Meier (KM) Plotter. Cancers were selected that showed survival data for 200 or more patients, to ensure greater reliability of data– this resulted in the analysis of 14 cancer subtypes (Table 3.1).

Using KM Plotter, of the 14 cancer subtypes included in this study, 11 cancer subtypes showed that high expression of KPNβ1 associated with poorer patient survival, of which, data from 6 cancer subtypes showed a significant correlation, namely, kidney renal papillary cell carcinoma, liver hepatocellular carcinoma, lung adenocarcinoma, sarcoma, thyroid carcinoma and uterine corpus endometrial carcinoma (Figure 3.5). Whilst 5 of the other cancer subtypes did not show a significant correlation, a general trend of higher KPNβ1 gene expression associating with poorer patient survival was observed (Figure 3.6). Interestingly, 3 of the remaining cancer subtypes within this dataset showed that a high expression of KPNβ1 associated with significantly better patient survival; kidney renal clear cell carcinoma, ovarian cancer and stomach adenocarcinoma (Figure 3.7).

The results of these Kaplan Meier plots highlight a possible link between KPNβ1 gene expression and patient survival, albeit some show a positive correlation while others show a negative correlation. Interestingly, more than 50% of the cancers show poorer patient survival when KPNβ1 is highly expressed, suggesting that KPNβ1 may serve as a survival biomarker in a cancer dependent manner.

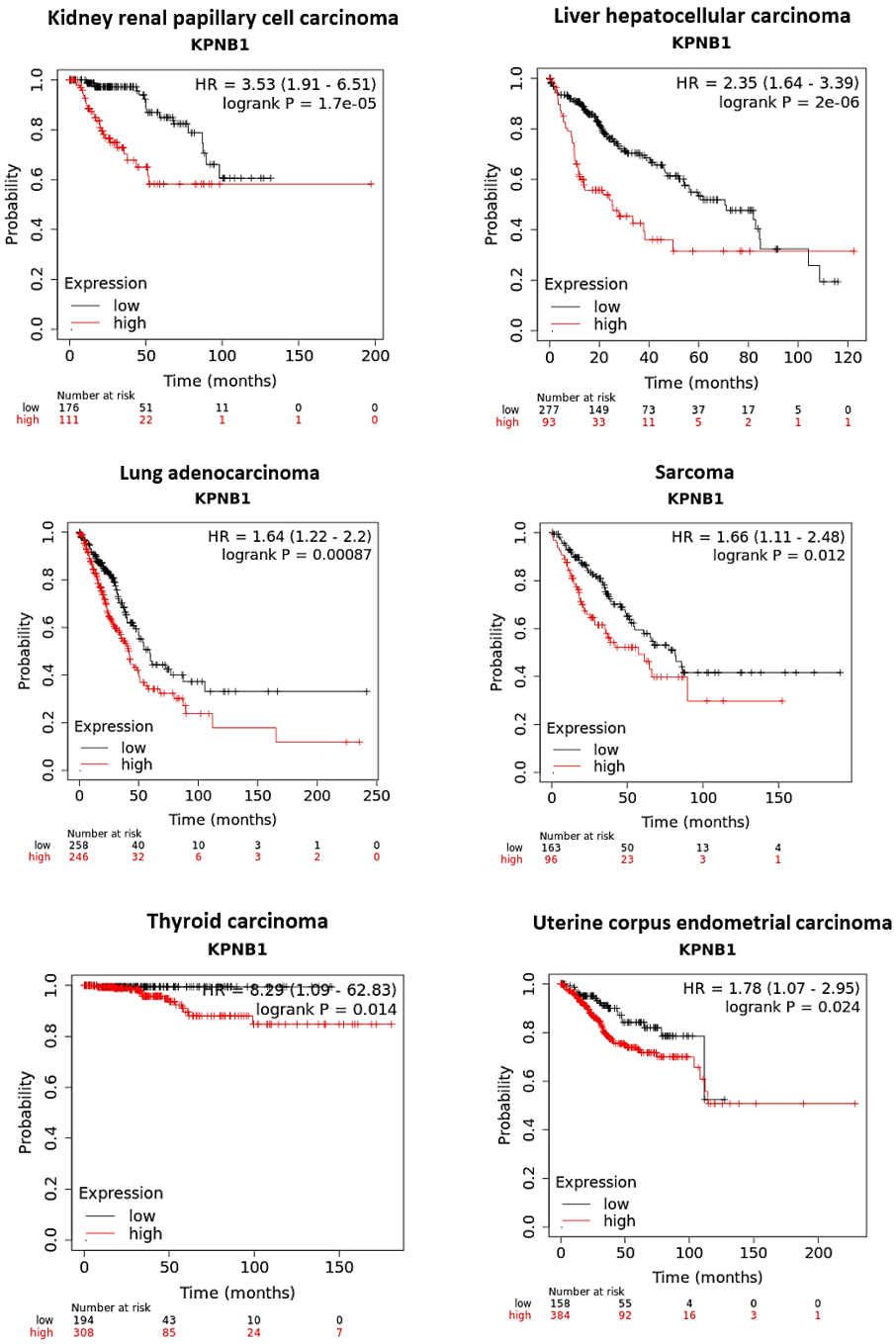

Figure 3.5. Association between higher KPNβ1 gene expression and significantly poorer patient survival. Kaplan Meier plots for cancer subtypes where high KPNβ1 gene expression shows a significant correlation with poorer patient survival. The red line indicates high KPNβ1 gene expression groups and the black line indicates the low KPNβ1 gene expression groups. Plots were obtained from a search conducted on KM plotter after splitting patients by auto select best cut-off and selecting cancer subtypes where n>200 ($p<0.05$ is considered statistically significant). HR indicates the hazard ratio, or the magnitude of the difference between the two curves.

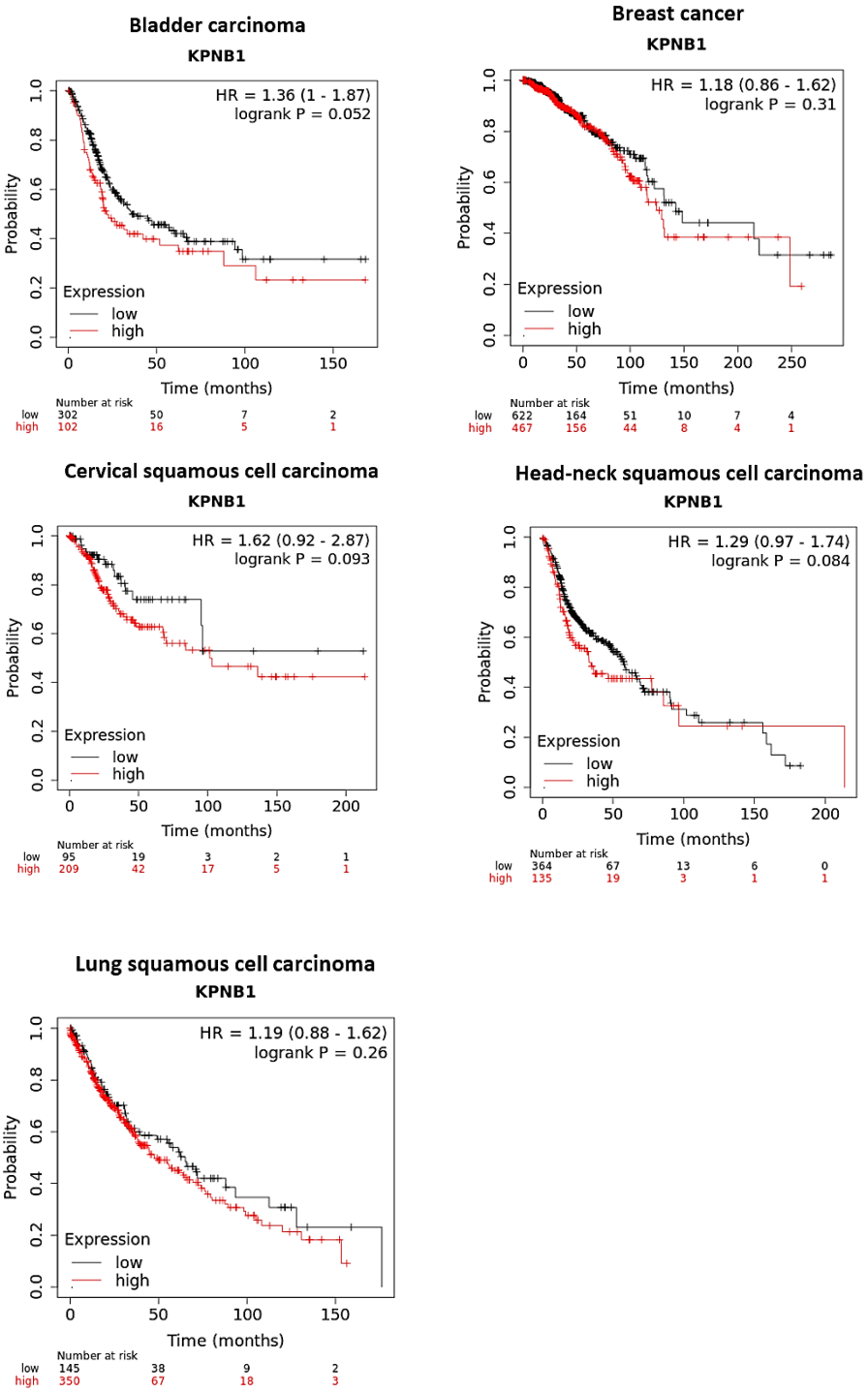

Figure 3.6. Association of higher KPNβ1 gene expression with no significant but a trend towards poorer patient survival. Kaplan Meier plots for cancer subtypes where high KPNβ1 gene expression shows a correlation with poorer patient survival, but is not significant. The red line indicates high KPNβ1 gene expression groups and the black line indicates the low KPNβ1 gene expression groups. Plots were obtained from a search conducted on KM plotter after splitting patients by auto select best cut-off and selecting cancer subtypes where n>200 ($p<0.05$ is considered statistically significant). HR indicates the hazard ratio, or the magnitude of the difference between the two curves.

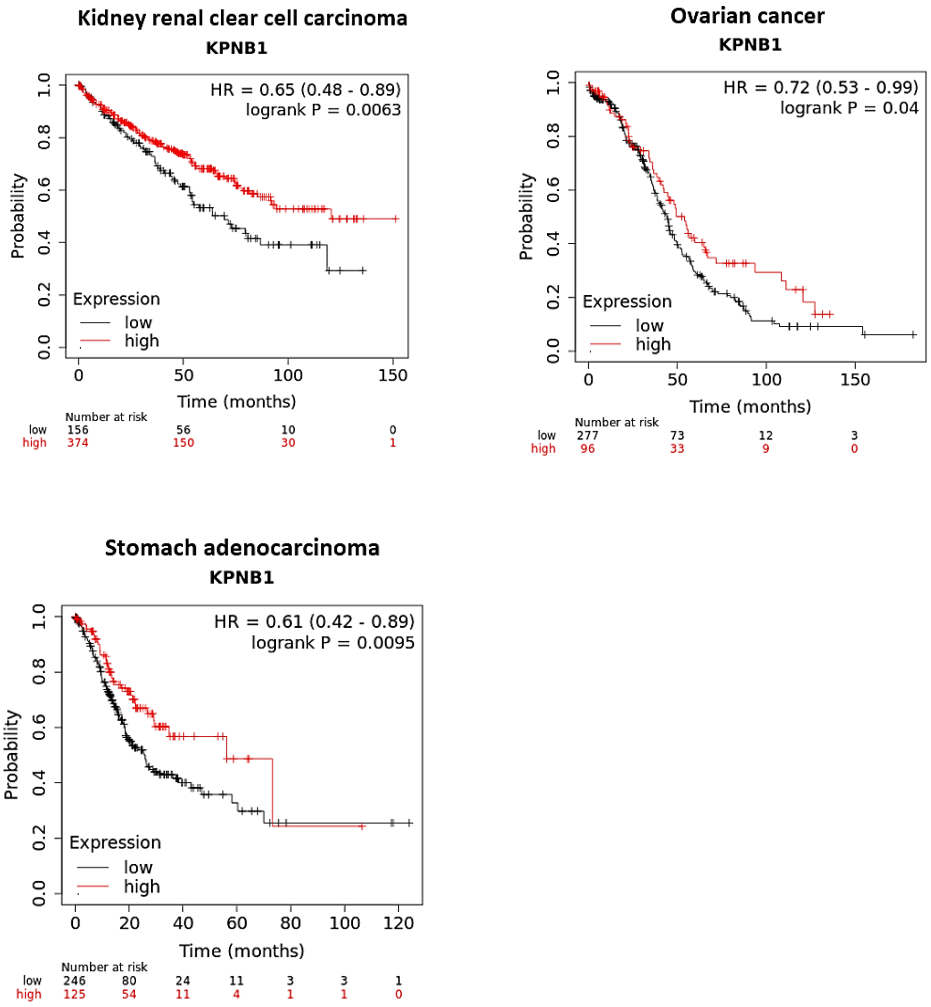

Figure 3.7. Association between high KPNβ1 gene expression and improved patient survival. Kaplan Meier plots for cancer subtypes where high KPNβ1 gene expression shows a significant correlation with better patient survival. Plots were obtained from a search conducted on KM plotter after splitting patients by auto select best cut-off and selecting cancer subtypes where n>200 ($p<0.05$ is considered statistically significant). HR indicates the hazard ratio, or the magnitude of the difference between the two curves.

Table 3.1 Summary of the number of patient samples that were used and the trend observed for each cancer subtype (n = number of patients with available clinical data).

Cancer subtype	n	Trend observed with high KPNβ1 gene expression
Kidney renal papillary cell carcinoma	288	Poorer patient survival
Liver hepatocellular carcinoma	371	Poorer patient survival
Lung adenocarcinoma	513	Poorer patient survival
Sarcoma	259	Poorer patient survival
Thyroid carcinoma	502	Poorer patient survival
Uterine corpus endometrial carcinoma	543	Poorer patient survival
Bladder carcinoma	405	No significant trend
Breast cancer	1090	No significant trend
Cervical squamous cell carcinoma	304	No significant trend
Head-neck squamous cell carcinoma	500	No significant trend
Lung squamous cell carcinoma	501	No significant trend
Kidney renal clear cell carcinoma	530	Improved patient survival
Ovarian cancer	374	Improved patient survival
Stomach adenocarcinoma	375	Improved patient survival

3.2.3 KPNβ1 protein expression in cancer cell lines compared to non-cancer of different tissue origin

After determining that KPNβ1 mRNA was overexpressed in cancer patient material using bioinformatic databases, and displayed associations with patient survival, we next investigated KPNβ1 expression at the proteomic level in chosen cultured cell lines of different tissue origin, using Western blotting. Protein was harvested from cells and Western blotting performed (Figure 3.8A), whereafter the expression of KPNβ1 in each cancer cell line was calculated relative to the loading control, β-Tubulin and then expressed relative to the non-cancer epithelial cell line, ARPE-19, after quantification of band intensities using ImageJ (Figure 3.8B). EPC2 and hTERT RPE-1 cells were also included in the panel of cell lines investigated, as these are non-cancer epithelial cell lines that have been immortalised with the telomerase (hTERT) gene. The results showed higher KPNβ1 is expression in majority of the cancer cell lines including SiHa, HeLa and ME180 cervical cancer cells, U2OS osteosarcoma cells, HT1080 fibrosarcoma cells, WHCO5 and KYSE30 oesophageal cancer cells, HepaRG liver cancer cells, KatoIII gastric cancer cells, MCF7 breast cancer cells and End1 transformed cervical epithelial cells. No difference in KPNβ1 levels was detected in T47D and MDA-MB-231 breast cancer cells in comparison to the non-cancer ARPE-19 cells. These results are in

line with the results obtained from the bioinformatic analyses, indicating that while most cancers analysed in this study show overexpression of KPNβ1, there are some deviations, which could likely be due to cancer heterogeneity and biological variations that exist within a tumour. Moreover, we also observed that an overexpression seen at the genomic level (mRNA) generally translates to an overexpression at the proteomic level.

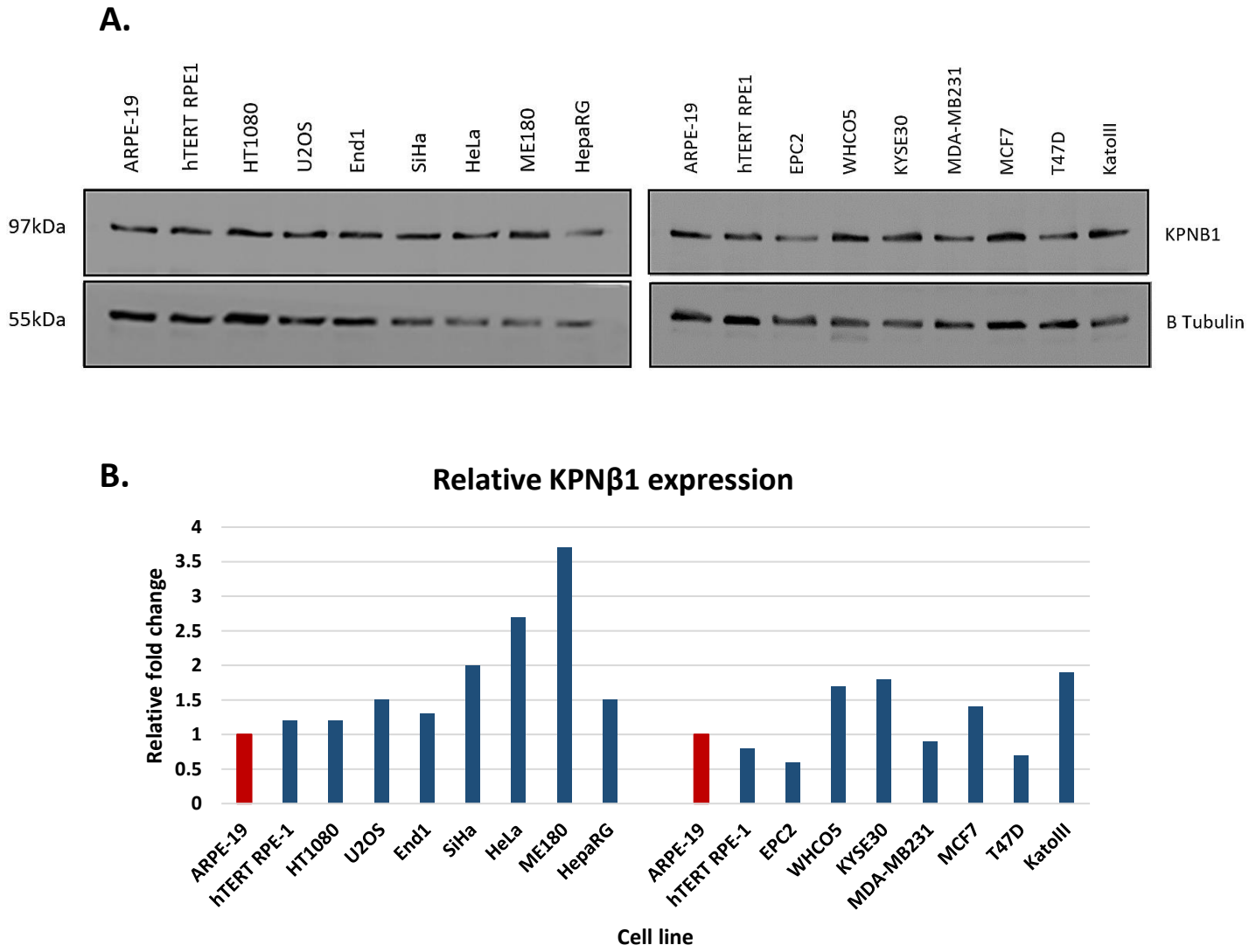

Figure 3.8. KPNβ1 protein expression in cancer and non-cancer cell lines. (A) A Western blot analysis showing KPNβ1 expression in cancer cell lines of different tissue types, using β Tubulin as the loading control. Results shown are representative of experiments performed two independent times (using two independent protein isolations). Similar results were obtained both times. (B) Bar chart showing the quantification of KPNβ1 levels relative to β-Tubulin, and expressed relative to the non-cancer cell line, ARPE-19. Results shown are the mean fold change of experiments performed using proteins lysates for each cell line from two independent isolations.

3.2.4 Investigating the effect of INI-43 on cancer and non-cancer cell viability

Having investigated KPNβ1 expression in cancer and non-cancer cell lines of different tissue origin, we next investigated the effect of INI-43 (an inhibitor of KPNβ1 associated nuclear import) on cell viability using MTT assays. MTT assays were performed in triplicate on cell lines of different tissue origin. Cells were treated with increasing concentrations of INI-43 in a 96-well plate for 48 hours and treated with MTT reagent to determine the number of viable cells. Results are displayed as Hill plots in Figure 3.9 and CC_{50} values for experiments performed in triplicate and repeated at least two independent times are tabulated in Table 3.2.

The results of the MTT assays showed that INI-43 induced cell death in both cancer and non-cancer cell lines. However, INI-43 was more effective at killing cancer, immortalised and transformed cell lines at concentrations that had little/no effect on the non-cancer cell line, ARPE-19 (Table 3.2). Overall, the cancer cell lines had CC_{50} values ranging from approximately 5 to 15 µM while the non-cancer cell line, ARPE-19 had an CC_{50} value of approximately 25 µM, at least two-fold higher than the CC_{50} values of majority of the cancer cell lines (Figure 3.10). This shows that the cancer cell lines tested in this study are more sensitive to INI-43 treatment than the non-cancer cell line with a Therapeutic Index (TI) ranging between 1.7 to 5. Other interesting observations included the fact that the highly aggressive and metastatic triple negative breast cancer cells, MDA-MB231, were more sensitive to INI-43 (with a lower CC_{50} value) compared to the less aggressive MCF7 and T47D breast cancer cells. Additionally, the results showed that the immortalised epithelial cell line, hTERT RPE-1 were more sensitive to INI-43 treatment compared to the non-immortalised ARPE-19 cells, suggesting that immortalisation itself may infer some cellular dependence on KPNβ1.

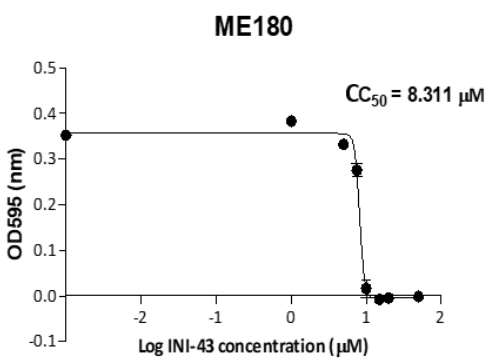
ME180
CC50 = 8.311 μM
OD595 (nm)
Log INI-43 concentration (μM)

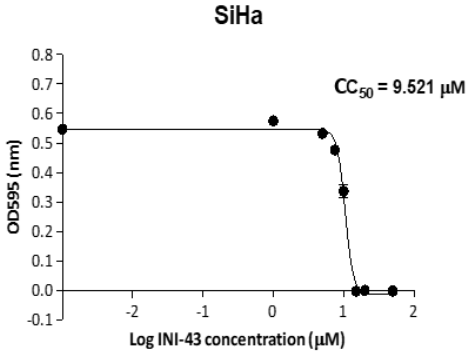
SiHa
CC50 = 9.521 μM
OD595 (nm)
Log INI-43 concentration (μM)

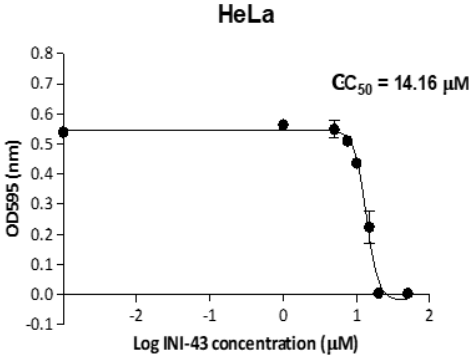
HeLa
CC50 = 14.16 μM
OD595 (nm)
Log INI-43 concentration (μM)

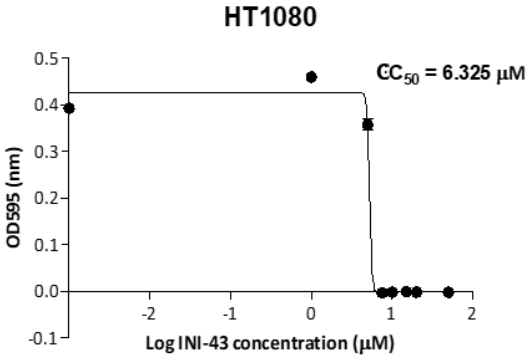
HT1080
CC50 = 6.325 μM
OD595 (nm)
Log INI-43 concentration (μM)

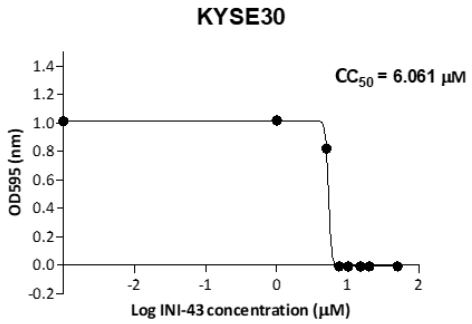
KYSE30
CC50 = 6.061 μM
OD595 (nm)
Log INI-43 concentration (μM)

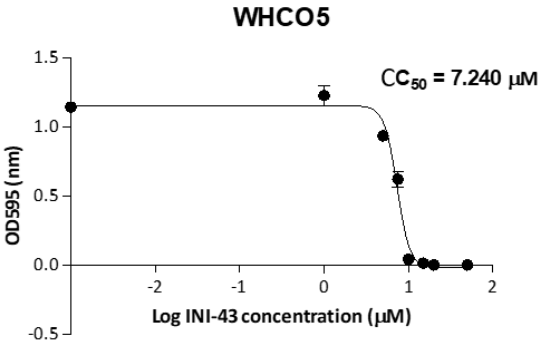
WHCO5
CC50 = 7.240 μM
OD595 (nm)
Log INI-43 concentration (μM)

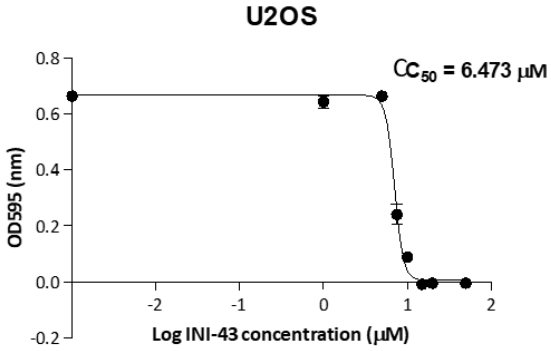
U2OS
CC50 = 6.473 μM
OD595 (nm)
Log INI-43 concentration (μM)

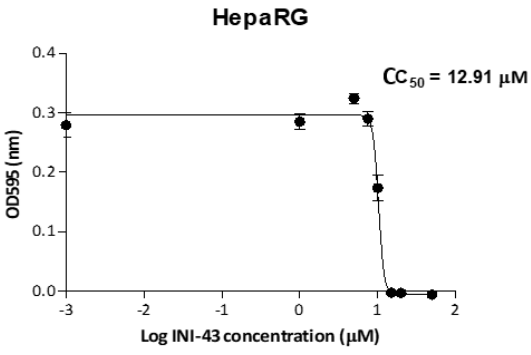
HepaRG
CC50 = 12.91 μM
OD595 (nm)
Log INI-43 concentration (μM)

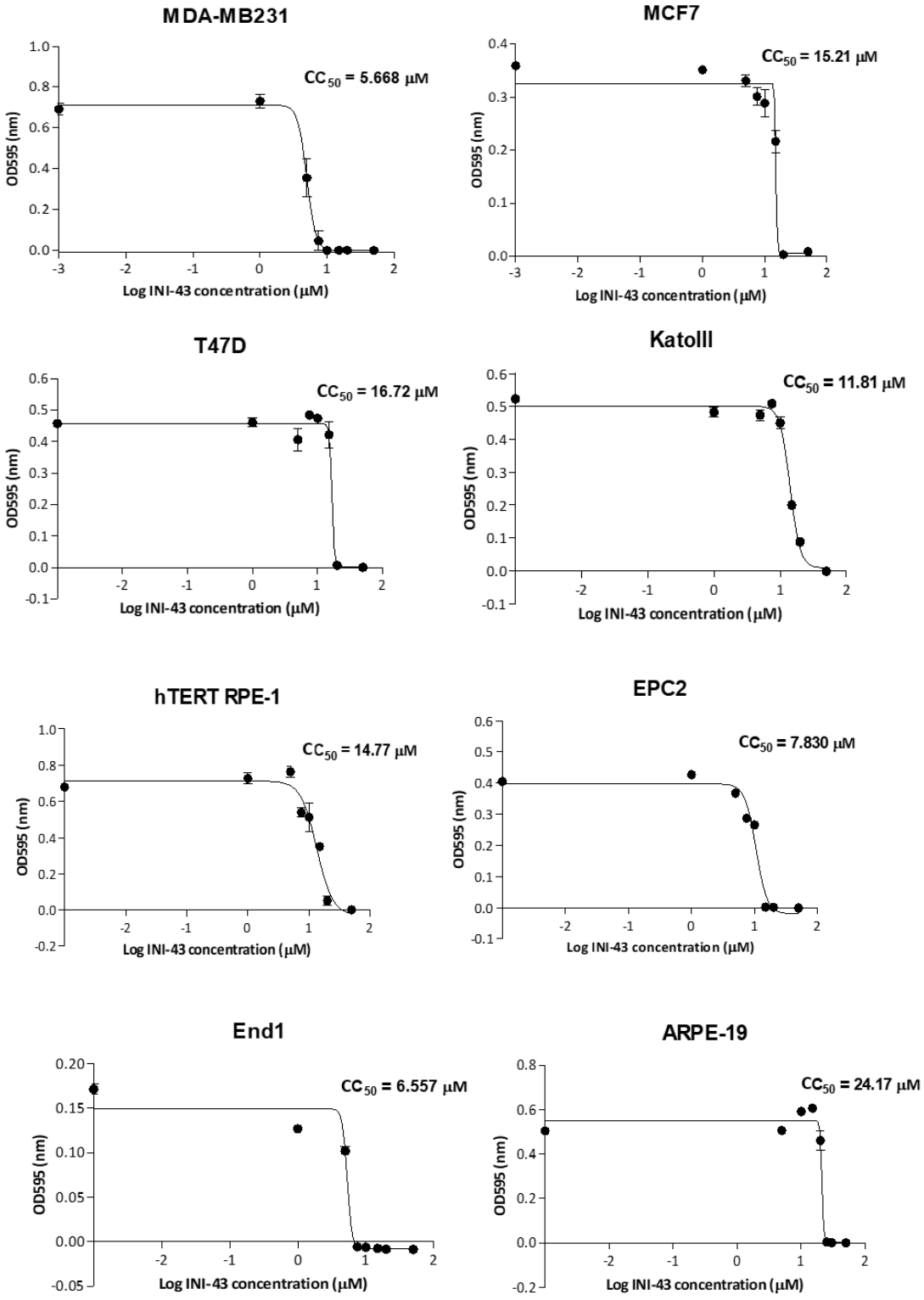

Figure 3.9. Representative hill plots for CC_{50} determination of INI-43 in cancer and non-cancer cell lines. All the cell lines were treated with increasing concentrations of INI-43 for 48 hours and cell viability was monitored using the MTT assay. Results shown are the mean ± SEM of experiments performed in triplicate and repeated at least two independent times.

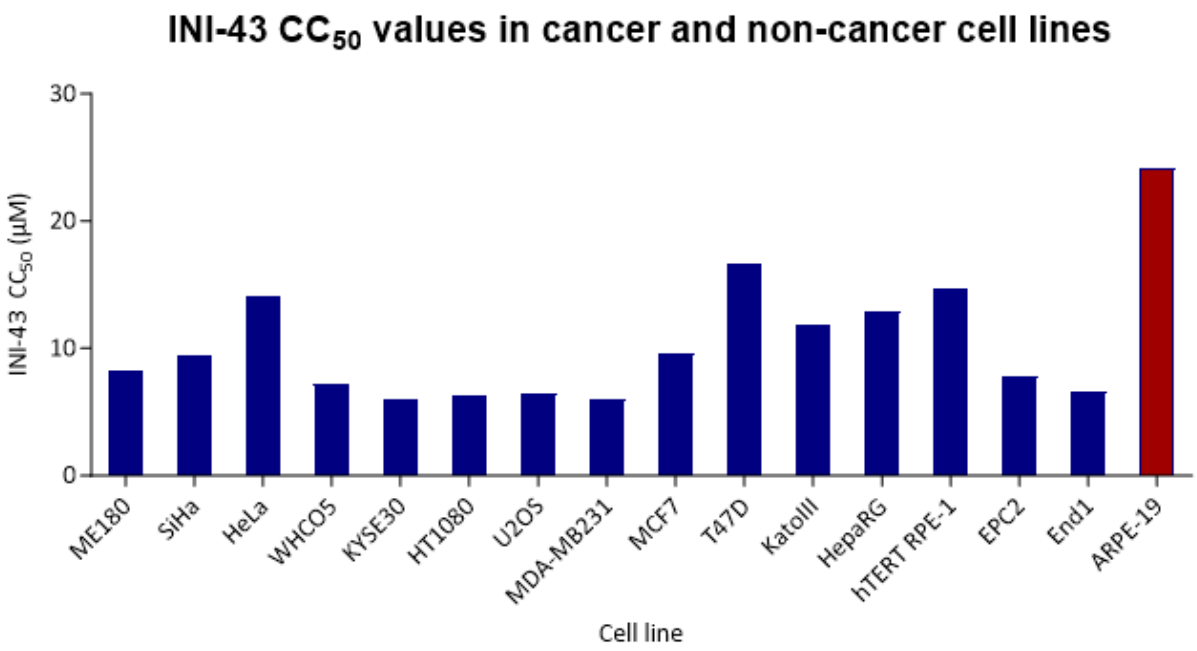

Figure 3.10. CC_{50} values of INI-43 in different cancer cell lines relative to the non-cancer cell line, ARPE-19. Bar graph showing comparison between CC_{50} values of INI-43 in cancer cell lines vs the non-cancer cell line, ARPE-19 shown in red. INI-43 was more cytotoxic to the cancer cell lines compared to the non-cancer cell line, ARPE-19. All experiments were performed in triplicate at least two independent times and the average CC_{50} value was plotted.

Table 3.2. Average CC_{50} values and 95% Confidence Intervals for INI-43 in cancer cell lines and the non-cancer cell line, ARPE-19.

Cancer type	Cell line	CC_{50} (µM)	95% Confidence Interval
Cervical	ME180	8.3	7.98 - 8.67
	SiHa	9.5	8.74 - 10.38
	HeLa	14.2	12.81 - 15.67
Breast	MDA-MB231	5.7	5.20 - 6.26
	MCF7	15.2	15.00 - 20.00
	T47D	16.7	14.22 - 19.98
Oesophageal	WHCO5	7.2	6.05 - 8.72
	KYSE30	6.1	5.49 - 6.69
Fibrosarcoma	HT1080	6.3	5.74 - 7.96
Osteosarcoma	U2OS	6.5	5.61 - 7.50
Gastric	KatoIII	11.8	10.44 - 13.37
Liver	HepaRG	12.9	10.03 - 16.90
Transformed	End1 (cervical)	6.6	4.91 - 8.76
Immortalised	hTERT RPE-1 (retinal)	14.8	10.58 - 20.67
	EPC2 (oesophageal)	7.8	6.42 - 9.62
Non-cancer	ARPE-19 (retinal)	24.2	19.71 - 30.53

3.2.5 Determining the mode of cell death following treatment with INI-43

After determining that INI-43 inhibited cell viability on a range of cancer cell lines of different tissue origin, we next determined the mode of cell death was via apoptosis. Apoptosis is a method of programmed cell death where the cells sense stressors either from within the cell

(intrinsic pathway) or from outside of the cell (extrinsic pathway) and induce cell death by activating proteins and enzymes, such as caspases (82). In our study, to determine if cells treated with INI-43 underwent cell death through apoptosis, we used the Caspase-Glo^{TM} 3/7 Assay on representative cancer cell lines; ME180 cervical cancer cells, HepaRG liver cancer cells, MDAMB-231 breast cancer cells and KYSE30 oesophageal cancer cells. In this assay, treating the cells with the Caspase-Glo^{TM} 3/7 reagent induces cell lysis, followed by cleavage of the Caspase substrate by active Caspases in the cells. This releases aminoluciferin which is consumed by luciferase present in the reagent, generating a luminescent glow (83). The results are quantified using a luminometer and the luminescence is proportional to Caspase 3/7 activity. The results showed that after treatment with 10 µM INI-43 for 24 hours, ME180, HepaRG and MDA-MB231 cell lines all showed significant cell death by apoptosis. KYSE30 cells were all dead after treatment at this concentration, hence were treated with 7.5 µM INI-43 and displayed significant Caspase-3/7 activity after treatment at 7.5 µM. Interestingly, MDA-MB231 and KYSE30 that are reported to be obtained from aggressive breast and oesophageal cancer appear showed the highest Caspase-3/7 activity, suggesting that these cell lines were more sensitive to INI-43 and underwent more cell death via apoptosis (Figure 3.11).

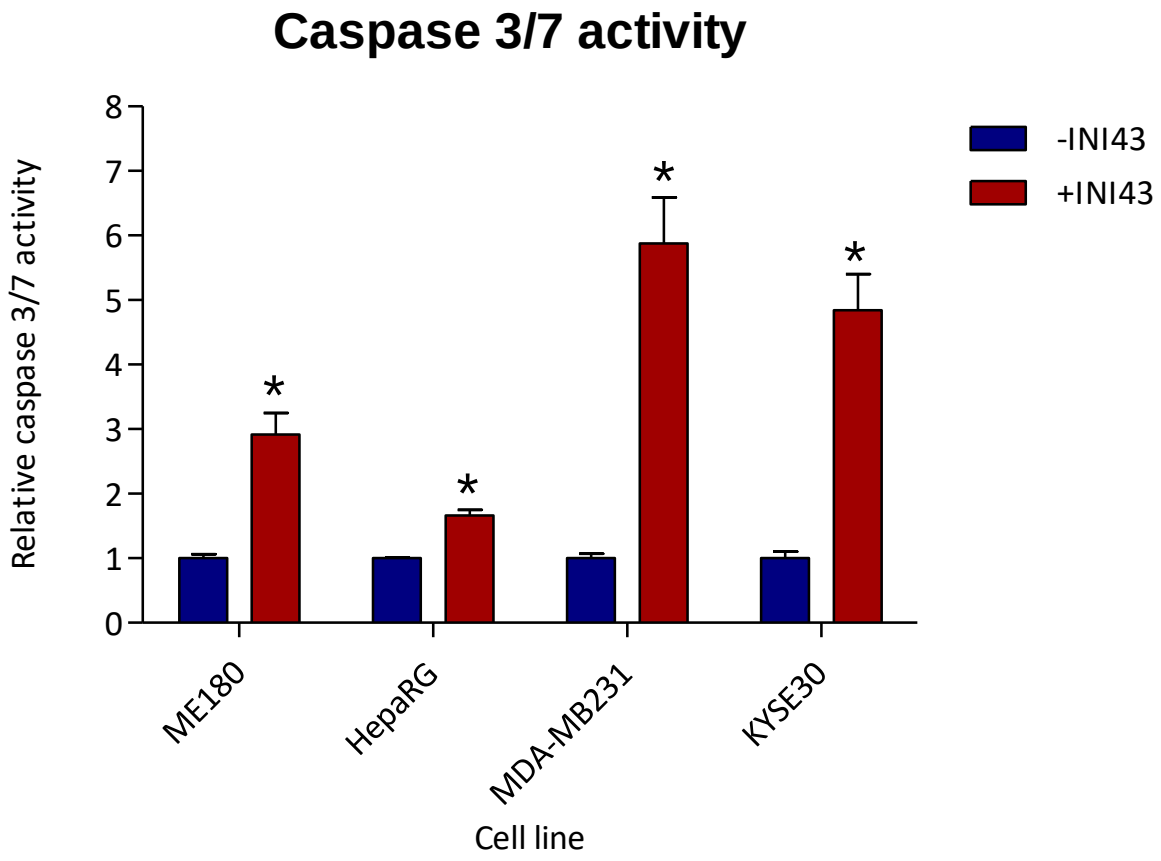

Figure 3.11. Treatment with INI-43 induces apoptosis in cancer cell lines. Caspase 3/7 activity was measured as an indicator of apoptosis in ME180, HepaRG, MDA-MB231 and KYSE30 cell lines after treatment with INI-43. Cells were treated with INI-43 for 24 hours after which the Caspase-Glo 3/7 assay was used to monitor apoptosis. Cells were all treated with 0 µM (shown as -INI43) and 10 µM (shown as +INI43) of INI-43, except for KYSE30 which was treated with 0 µM and 7.5 µM as 10 µM showed complete cell death. Results shown are the mean ± SEM of independent experiments performed in triplicate. Each independent experiment was repeated at least two times (*$p<0.05$).

3.3 Discussion

In this chapter, bioinformatic analyses revealed that KPNβ1 is overexpressed in various cancers at the genomic level, and that KPNβ1 expression levels associate with patient survival. Western blot analysis confirmed high levels of KPNβ1 protein in cancer cell lines of various origin. We further report that inhibiting KPNβ1 with the small molecule inhibitor, INI-43, has a greater cytotoxic effect on cancer cells compared to non-cancer cells, and INI-43 treatment results in cell death via apoptosis.

The overexpression of KPNβ1 mRNA and protein seen in multiple cancer types in this study, is in line with other published studies as highlighted in Table 1.2, including breast cancer, cervical cancer and gastric cancer, among others. Overexpression of KPNβ1 is hypothesised to increase the nuclear import efficiency of cargo molecules into the nucleus and is suggested to maintain the higher metabolic demand of cancer cells (6). Furthermore, the association of KPNβ1 expression with patient survival reported in this study is very interesting as it may aid in predicting patient prognosis or diagnosis by studying the KPNβ1 expression levels in patients. To our knowledge, this is the first study to report an association between KPNβ1 expression and patient survival in most of the cancer types investigated. However, it should be kept in mind that using different online platforms for bioinformatic analysis may lead to some level of variability as different online platforms contain varying sets of data from different patients. For example; in our study, we used KM Plotter, which is an online platform that harbours data from GEO, EGA and TCGA and it showed that ovarian cancer patients with lower expression of KPNβ1 had poorer survival while Kodama et al. (2017) used GEO (using the publicly available GSE9891 dataset) and reported that ovarian cancer patients with higher expression of KPNβ1 had poorer prognosis (28). This highlights that even though there is overlap between the two datasets from GEO, the patient datasets from KM Plotter have additional information from EGA and TCGA making the datasets different, and varying results may arise due to cancer heterogeneity. Overall, however, our results were consistent in most cases and showed that for the majority of cancer types, high expression of KPNβ1 associated with poorer patient survival.

In this chapter, we also reported that INI-43 has a greater cell killing effect on cancer cells compared to non-cancer cells, with a Therapeutic Index (TI) ranging between 1.7 to 5. TI is a measure of the relative safety of a drug, where a drug with a higher TI value is considered to be safe, and TI's less than 3 generally require the drug to be dosed carefully (84). TI values of 1.7-5 for INI-43 suggest that INI-43 doses need to be monitored in some cancers should it be developed further.

There are published studies in literature that show that targeting other members of the nuclear transport protein family have anti-cancer effects. For example, the nuclear export protein, CRM1 was shown to be overexpressed in multiple cancers (Table 1.2), and targeting and inhibiting CRM1 showed greater cytotoxic effects in cancer cells compared to non-cancer cells (85). A nuclear export inhibitor of CRM1 is the natural compound, Leptomycin B that functions by targeting the 528 Cysteine residue (in the mammalian system) in the NES-binding groove, preventing nuclear export (86). More recently, another group of inhibitors of increasing interest are the SINE (selective inhibitors of nuclear export) compounds, which have progressed into clinical trials. This water-soluble series of drugs target the same region as LMB but does so with reduced toxicity, enabling nuclear export to be blocked and the targeted killing of cancer cells (87). The most common SINE, Selinexor, has shown promise as a targeted anti-cancer agent. Selinexor has been tested in over 40 clinical trials and received FDA approval in the treatment of relapsed or refractory multiple myeloma in combination with dexamethasone (88–90). Furthermore, Selinexor was seen to be highly effective against prostate cancer in mouse models (91). This shows the potential of targeting and inhibiting nuclear transport proteins as a therapeutic strategy.

While other nuclear transport proteins and inhibitors that target nuclear export have been studied extensively, only a few inhibitors of nuclear import via KPNβ1 have been studied thus far, including INI-43, Importazole and Karyostatin 1A. Another inhibitor that has been studied and is aimed at KPNα2 is the FDA-approved antiparasitic agent, Ivermectin, albeit that Ivermectin does not necessarily target KPNα2 only. Advantageously, inhibiting KPNβ1 or its adapter protein, KPNα2 will both block the KPNβ1 import pathway since KPNβ1 may either

function on its own or through the aid of KPNα2. In a study done by van der Watt et al. (2016) using an NFAT assay to compare the inhibitors; INI-43, Ivermectin and Importazole, it was reported that INI-43 was the more potent inhibitor of nuclear transport (70). Together our findings in this chapter provides evidence that KPNβ1 is a promising diagnostic/prognostic marker for a broad range of cancer types and that the nuclear import inhibitor, INI-43 has potential as an anti-cancer agent that targets nuclear import pathways that cancer cells rely on.

Chapter 4

Investigating the engagement between INI-43 and nuclear transport proteins

4.1 Introduction

It is important that a drug binds to its cognate target protein because binding of a drug to any other proteins may lead to unwanted side effects and lack of efficacy in patients (75). In the previous chapter, we reported that INI-43, a drug that was computationally designed to target KPNβ1, was more cytotoxic to cancer cells compared to non-cancer cells. In this chapter, we aimed to determine if INI-43 in fact exerts those effects by targeting KPNβ1. We used the Cellular Thermal Shift Assay (CETSA) using cervical cancer cells as the model system.

The Cellular Thermal Shift Assay is a target engagement assay that has emerged as a useful tool in recent years. This assay assesses any shifts in thermal stability of proteins upon compound binding. It is based on the principle that upon heating intact cells, proteins will denature and aggregate at elevated temperatures. Ligand-bound proteins, on the other hand, remain in solution. The denatured and aggregated proteins are removed by centrifugation and the relative amount of remaining soluble protein, at the various temperatures, is measured using Western blots. Results are plotted against temperature to generate a melt curve. If the compound has engaged with the protein, the thermal stability of the protein will be altered, and a shift will be noticed in the melt curve (Figure 4.1). Binding of a compound to a protein may either stabilise the protein target resulting in a shift in the melt curve to the right side of the untreated protein group or it may destabilise the protein target leading to a shift in the melt curve to the left side of the untreated protein group (92–95). This shift in the melt curve confirms target engagement. CETSA's can be conducted on intact cells or on cell lysates. It is an advantageous assay because in the case of intact cells, proteins can be studied in live cells in their normal cellular and physiological environment without the need for any modifications such as protein purification (96). Therefore, CETSA's can be used in the drug discovery pipeline to confirm target engagement between a drug and its hypothesised target.

A.

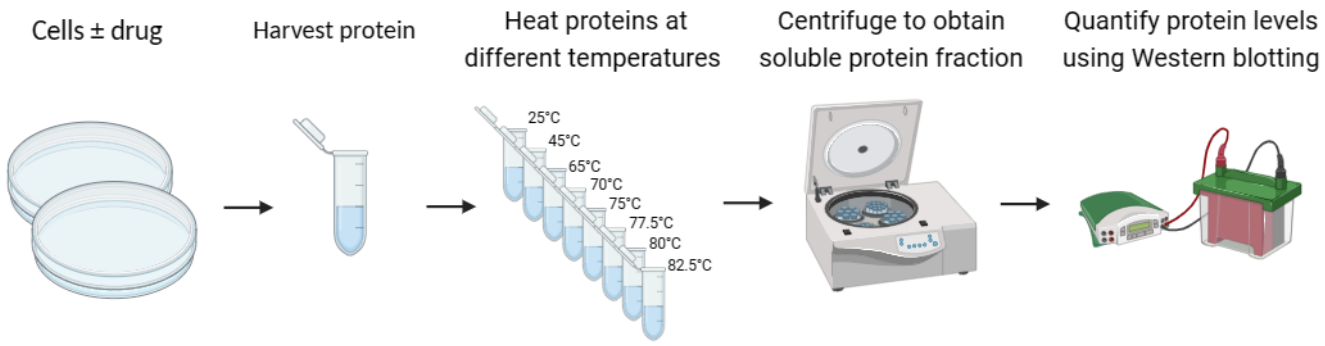

B.

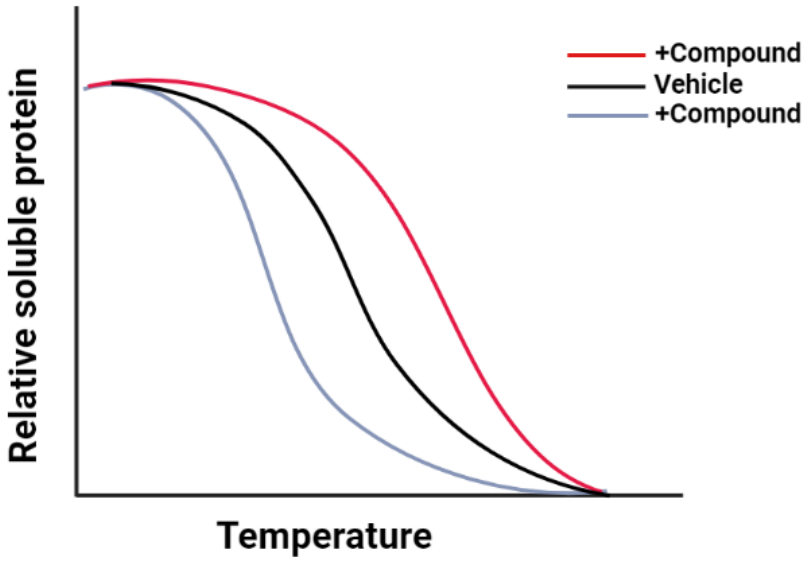

Figure 4.1. Diagrammatic representation of CETSA experimental flow and melt cures following target engagement. (A) CETSA experimental design. (B) Binding of a compound to a target may either stabilise it resulting in a right-shifted melt curve (indicated in red) or destabilise it resulting in a left-shifted melt curve (indicated in blue). A shift in the melt curve between compound and vehicle group indicates target engagement. Images were drawn using BioRender.

In this chapter, we aim to determine if INI-43 binds to KPNβ1 in intact cells using CETSA. Furthermore, we also aim to determine if INI-43 interacts with other members of the nuclear transport family, including some that have been reported to be overexpressed in certain cancers.

4.2 Results

4.2.1 Monitoring the uptake of INI-43 in intact HeLa cells

In order to design our CETSA experiments, we first wanted to investigate the timepoint at which INI-43 is taken up into cells. Since INI-43 is a fluorescent compound, uptake could be measured by fluorescence microscopy. We treated HeLa cells with 10 µM of INI-43 for up to 5 hours (a concentration of INI-43 below its CC_{50} so as not to immediately kill the cells), captured images using fluorescent microscopy and quantified the fluorescent signal from fifty different cells at different timepoints using ImageJ. The results show that INI-43 is taken up into the cells relatively quickly, with maximal uptake already taking place within the first hour and a half of treatment and plateauing shortly thereafter (Figure 4.2). From this experiment, it was established that a short treatment time of between 1.5 and 3 hours was sufficient for INI-43 uptake and could be used for subsequent CETSA experiments.

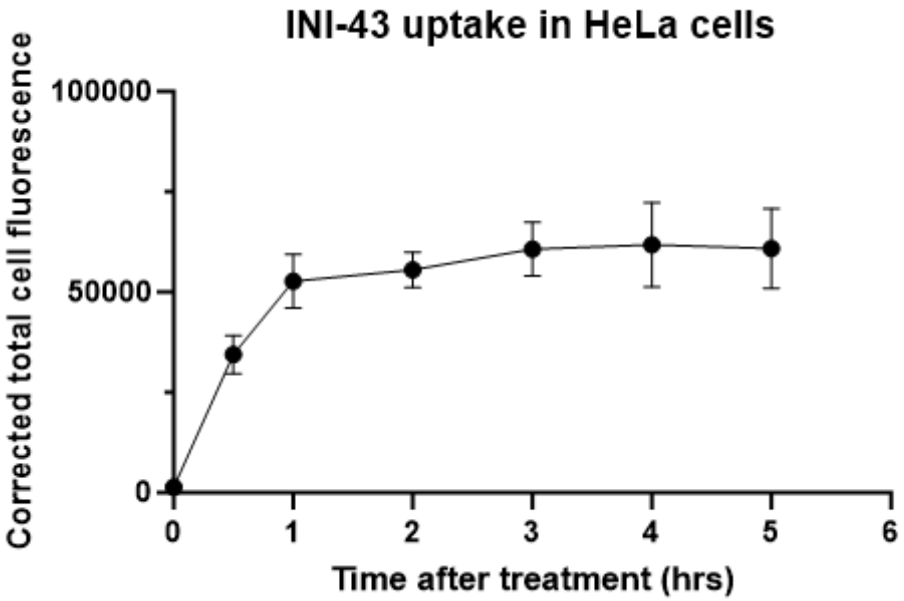

Figure 4.2. Time-dependent uptake of INI-43 into HeLa cells. To determine when INI-43 is taken up into HeLa cervical cancer cells, cells were treated with 10 µM of INI-43 for up to 5 hours and the fluorescent signal from fifty different cells were detected and quantified at chosen timepoints using ImageJ. Fluorescence was plotted as corrected total cell fluorescence (CTCF) to account for any background fluorescence given off in the samples where CTCF = Integrated Density – (Area of selected cell X Mean fluorescence of background readings). Results shown are the mean ± SEM. Maximal uptake of INI-43 occurs within the first hour and a half of treatment.

4.2.2 Cellular Thermal Shift Assay experimental design

To determine the optimal conditions for the CETSA experiment, it was first necessary to determine the temperature range that would result in KPNβ1 degradation. HeLa cells were treated with 10 µM of INI-43 for 1.5 hours. Protein was then harvested from untreated and INI-43-treated cells, aliquoted into separated tubes, and subjected to various temperatures ranging from 25°C - 65°C. After Western blot analysis to analyse KPNβ1 levels at the different temperatures, a melt curve was generated (Figure 4.3A). The result showed that KPNβ1 was still relatively stable at 65°C, therefore, higher temperatures were included to monitor KPNβ1 degradation. A repeat experiment was performed, using temperatures ranging from 65°C – 85°C. Furthermore, the treatment time with INI-43 was extended to 3 hours, to ensure sufficient time for INI-43 to be taken up and exert its effects. With these conditions, KPNβ1 degradation was observed at the higher temperatures (Figure 4.3 B). The result also showed that INI-43 treatment of HeLa cells appeared to result in a right-handed shift in the melt curve, with KPNβ1 appearing to be stabilised upon INI-43 treatment. It was therefore decided to use these treatment conditions and subject treated and untreated cells to temperatures ranging from 25°C to 85°C so that a broader melt curve could be determined. Furthermore, the treatment time with INI-43 was extended to 3 hours, to ensure sufficient time for INI-43 to be taken up and exert its effects.

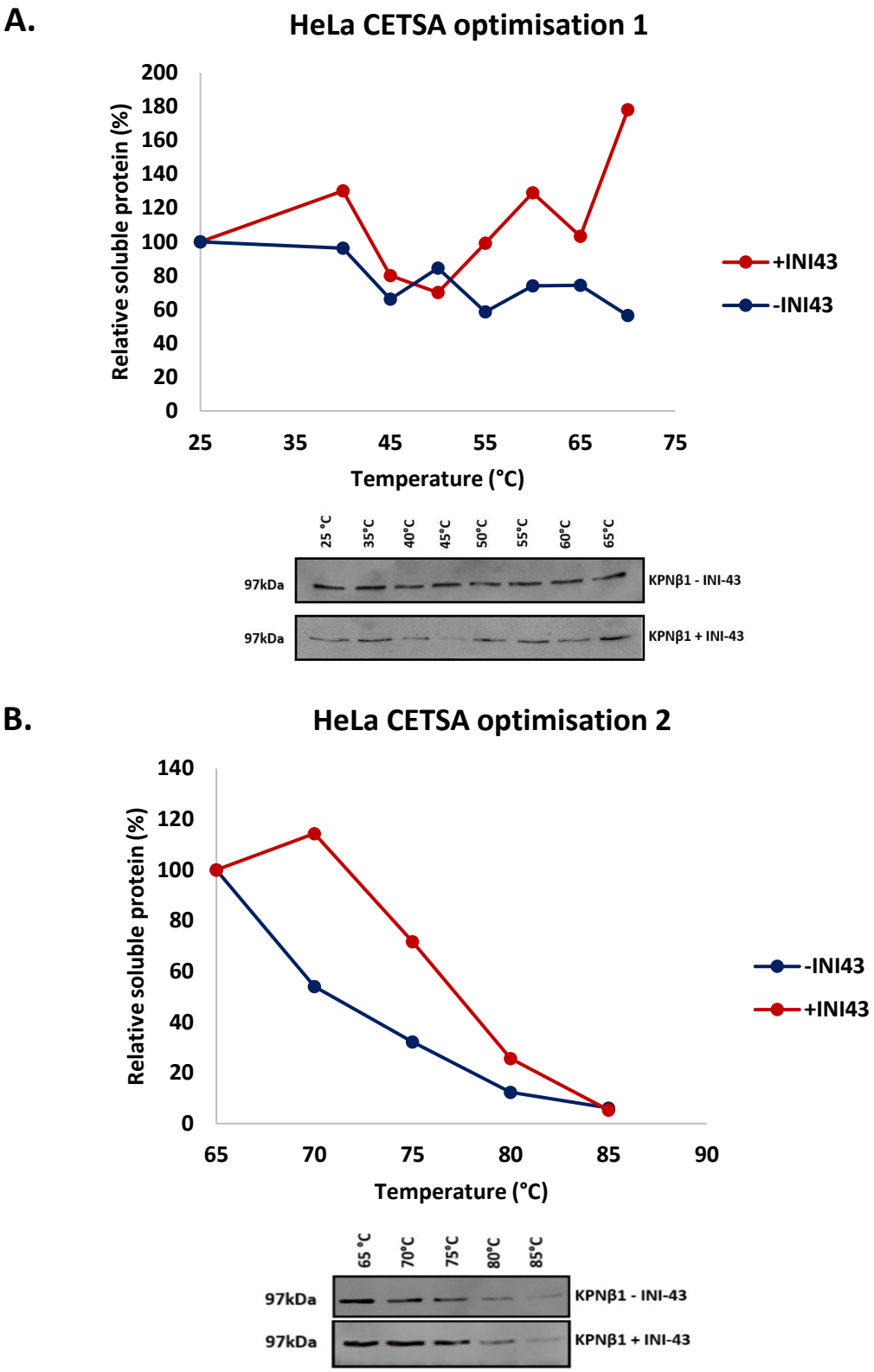

Figure 4.3. Thermal melt curves for CETSA optimisation experiments. Intact HeLa cells were treated with (A) 10 µM of INI-43 for 1.5 hours, protein harvested and heated at 25°C - 65°C and (B) 10 µM of INI-43 for 3 hours, protein harvested and heated at 65°C - 85°C. Relative soluble protein (%) was calculated as each band expressed relative to the starting temperature band (25°C for A and 65°C for B) on each respective blot. Immunoblots for the thermal melt curves are shown below their respective curves.

4.2.3 Investigating if INI-43 binds to KPNβ1 in intact cells

After finalising the experimental conditions, CETSA's were conducted on intact cells using the cervical cancer cell lines, HeLa, SiHa and ME180. Cells were treated in the presence and absence of INI-43 for 3 hours and exposed to different temperatures ranging from 25°C to 82.5°C. The relative soluble protein was then analysed by Western blotting for KPNβ1 levels and band intensity quantified to draw the thermal melt curves. The thermal melt curves were used to determine if any shift was observed between the control (-INI43) and the experimental (+INI43) groups, as a shift would confirm that INI-43 binds to KPNβ1.

The results of the thermal melt curve of KPNβ1 in HeLa cells (Figure 4.4 A) revealed a shift between the control (-INI43) and the experimental (+INI43) groups, where at 77.5°C there was a significant difference between the percentage of soluble KPNβ1 protein in untreated and INI-43 treated HeLa cells. More specifically, a right-handed shift was observed indicating that INI-43 has a stabilisation effect upon binding to KPNβ1, as higher temperatures were required to degrade the KPNβ1+INI43 experimental complex compared to the untreated KPNβ1 control, causing the right-handed shift. The experiment was repeated using SiHa and ME180 cervical cancer cell lines treated with INI-43, and similar results were obtained, confirming that the stabilisation effect of INI-43 on KPNβ1 is not specific to one cell line, but is apparent across different cell lines (Figure 4.4 B - C). Although the results in SiHa and ME180 cell lines showed the same findings, the significance could not be calculated as the experiments were repeated two independent times and not three times.

A.

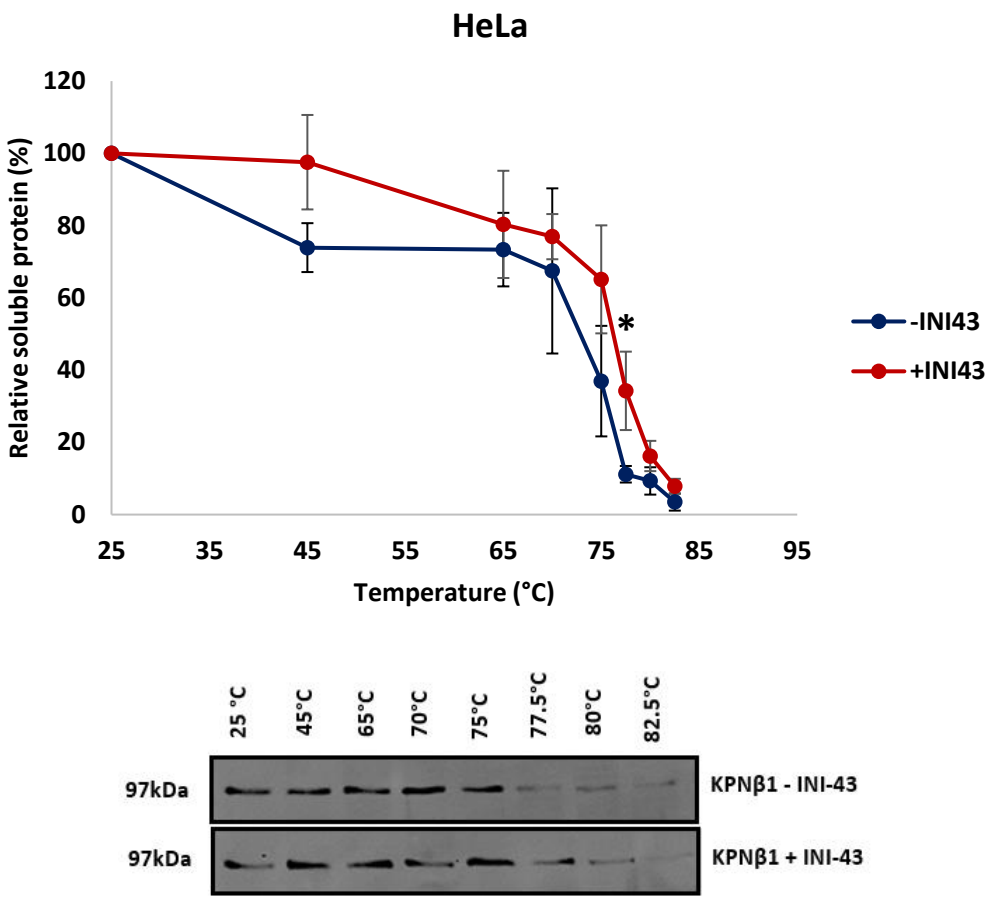
HeLa
Relative soluble protein (%)
120
100
80
60
40
20
0
25
35
45
55
65
75
85
95
Temperature (°C)
*
-INI43
+INI43
25 °C
45°C
65°C
70°C
75°C
77.5°C
80°C
82.5°C
97kDa
KPNβ1 - INI-43
97kDa
KPNβ1 + INI-43

B.

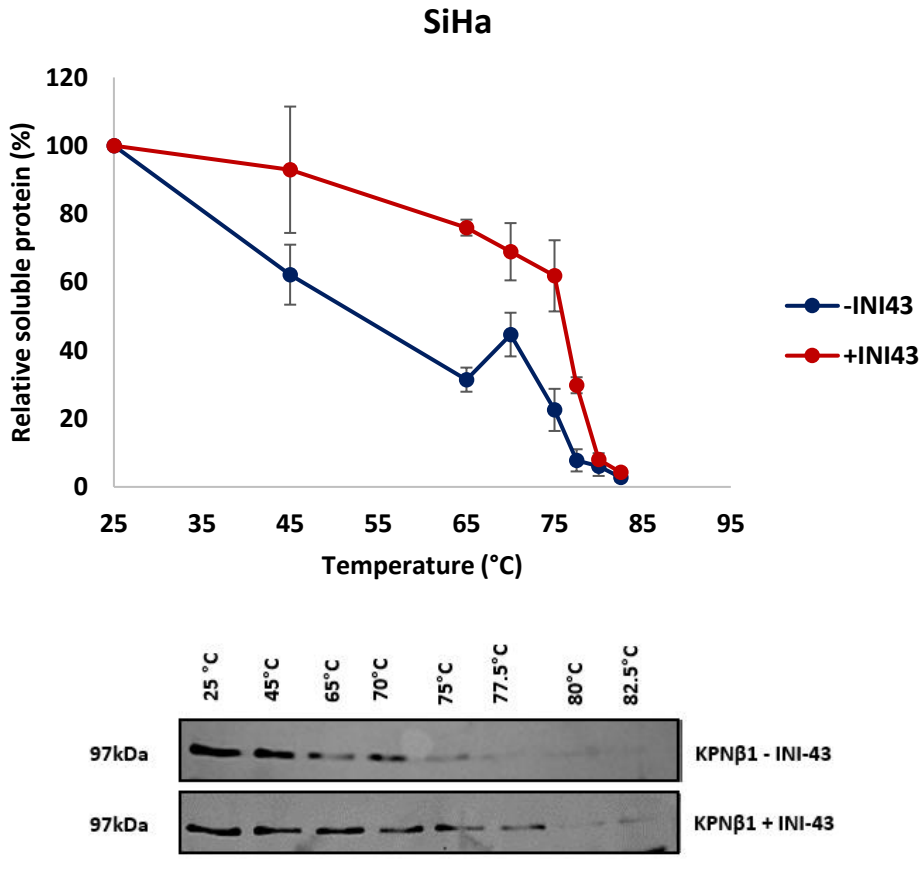
SiHa
Relative soluble protein (%)
120
100
80
60
40
20
0
25
35
45
55
65
75
85
95
Temperature (°C)
-INI43
+INI43
25 °C
45°C
65°C
70°C
75°C
77.5°C
80°C
82.5°C
97kDa
KPNβ1 - INI-43
97kDa
KPNβ1 + INI-43

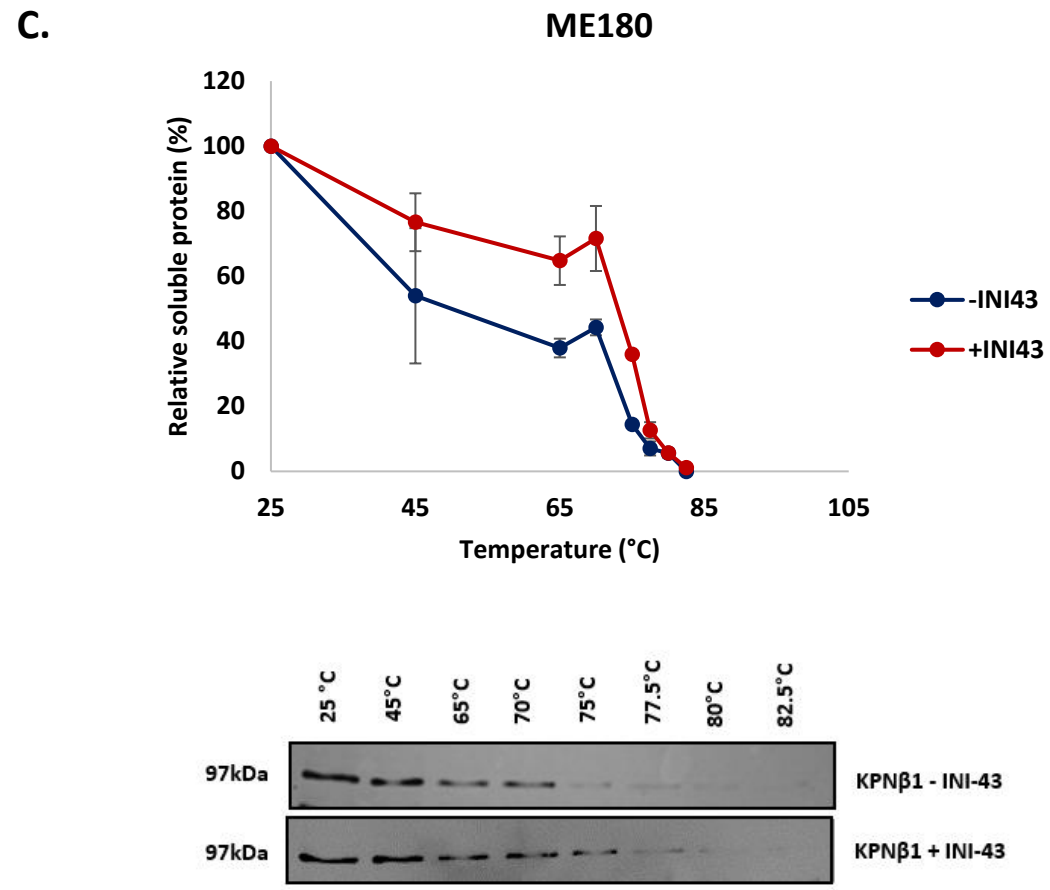

Figure 4.4. Thermal melt curves of CETSA experiments for KPNβ1 after treatment with INI-43 in intact cells. Cells were treated with 10 µM of INI-43 for 3 hours, protein harvested and treated at different temperatures to draw thermal melt curves for (A) HeLa, (B) SiHa and (C) ME180. Relative soluble protein (%) was calculated as each band expressed relative to the 25°C band on each respective blot. Representative immunoblots of each thermal melt curve are shown below their respective curves. HeLa experiments were performed three independent times and SiHa and ME180 were performed two independent times (*p<0.05).

4.2.4 Investigating if INI-43 binds to other members of the Karyopherin protein family

After determining that INI-43 stabilises KPNβ1 protein levels in cervical cancer cells, we next investigated whether INI-43 binds to other nuclear transport proteins that have been previously studied in our laboratory, including nuclear export proteins CAS and CRM1, nuclear import proteins IPO5 and TNPO1, and the KPNβ1 adapter protein, KPNα2. GAPDH levels were also determined, as the negative control as it is not a member of the Karyopherin superfamily. HeLa cells were treated in the presence or absence of INI-43 for 3 hours and exposed to temperatures ranging from 25°C to 82.5°C. The relative soluble protein was then quantified, using antibodies specific for each protein and thermal melt curves determined.

The results of the CETSA thermal melt curves (Figure 4.5 to 4.8) showed that all of the proteins were degraded, as temperatures were increased, and to varying extents. Importantly, the results showed that INI-43 does not appear to bind CAS, CRM1, KPNα2, TNPO1 and GAPDH to exert its cytotoxic effects because no shift was observed between the control (-INI43) and the experimental (+INI43) groups for these proteins (Figure 4.5, 4.6, 4.7). Interestingly, however, it appeared that INI-43 binds to the nuclear import protein, IPO5, as a right-handed shift was seen between the control (-INI43) and the experimental (+INI43) groups in the IPO5 thermal melt curve (Figure 4.8). The results of these CETSA's for the proteins analysed suggest that INI-43 is relatively specific for targeting KPNβ1, with the exception of IPO5, from the panel of nuclear transport proteins tested.

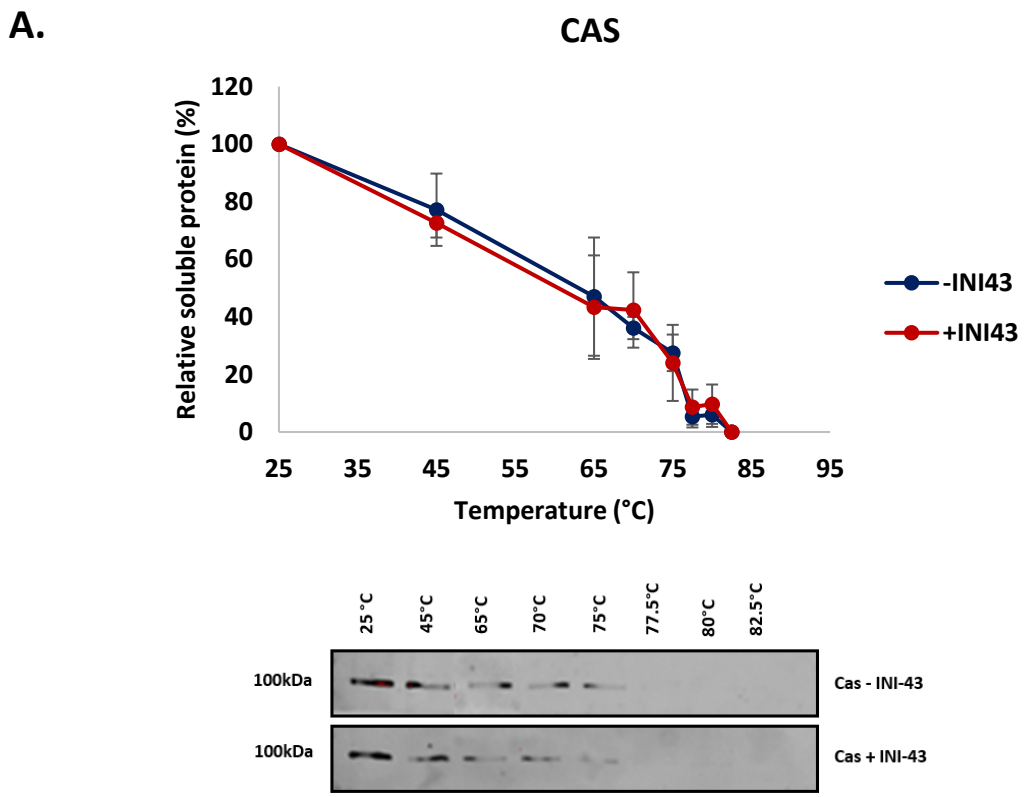

B.

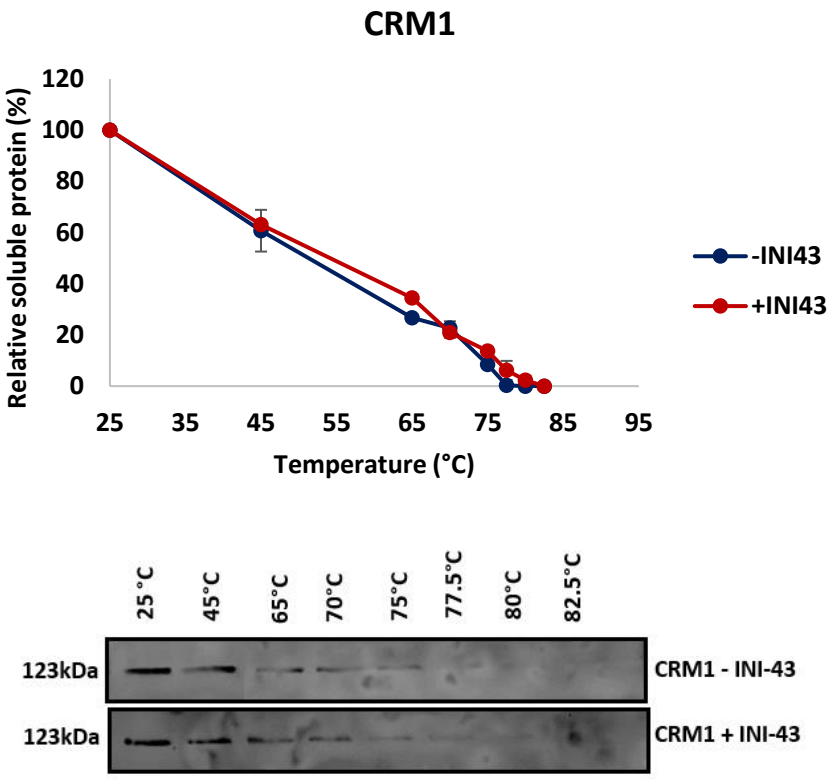

Figure 4.5. Thermal melt curves for nuclear export proteins showing no association with INI-43 in intact HeLa cells. HeLa cells were treated with 10 µM of INI-43 for 3 hours and treated at different temperatures to draw thermal melt curves for (A) CAS and (B) CRM1. Relative soluble protein (%) was calculated as each band expressed relative to the 25°C band on each respective blot. Representative immunoblots of each thermal melt curve are shown below their respective protein curves. Results shown are the mean ± SEM of experiments performed two independent times. Significance could not be calculated for these experiments as they were performed two independent times.

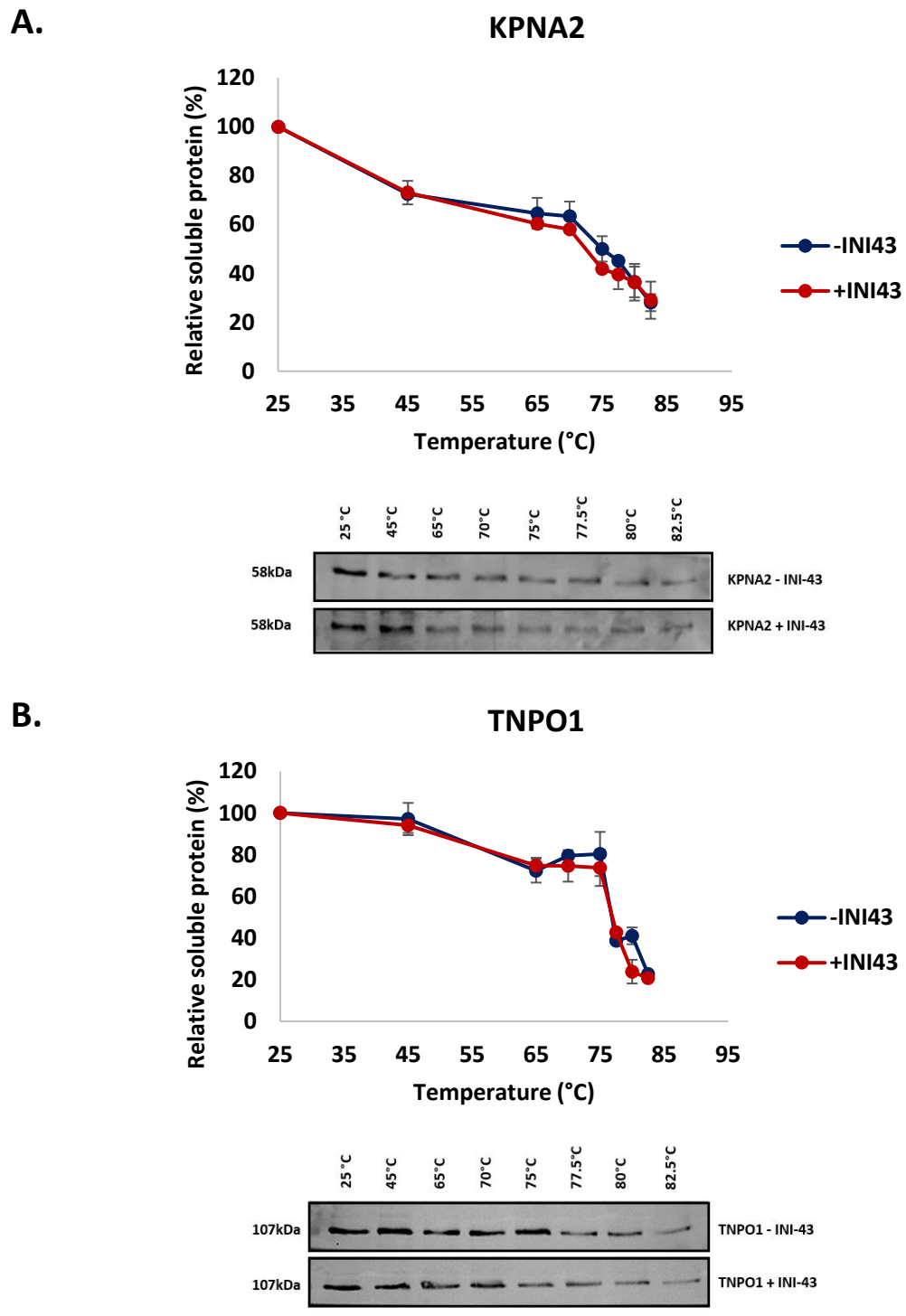

Figure 4.6. Thermal melt curves for nuclear import proteins showing no association with INI-43 in intact HeLa cells. HeLa cells were treated with 10 µM of INI-43 for 3 hours and treated at different temperatures to draw thermal melt curves for (A) KPNα2 and (B) TNPO1. Relative soluble protein (%) was calculated as each band expressed relative to the 25°C band on each respective blot. Representative immunoblots of each thermal melt curve are shown below their respective protein curves. Results shown are the mean ± SEM of experiments performed two independent times. Significance could not be calculated for these experiments as they were performed two independent times.

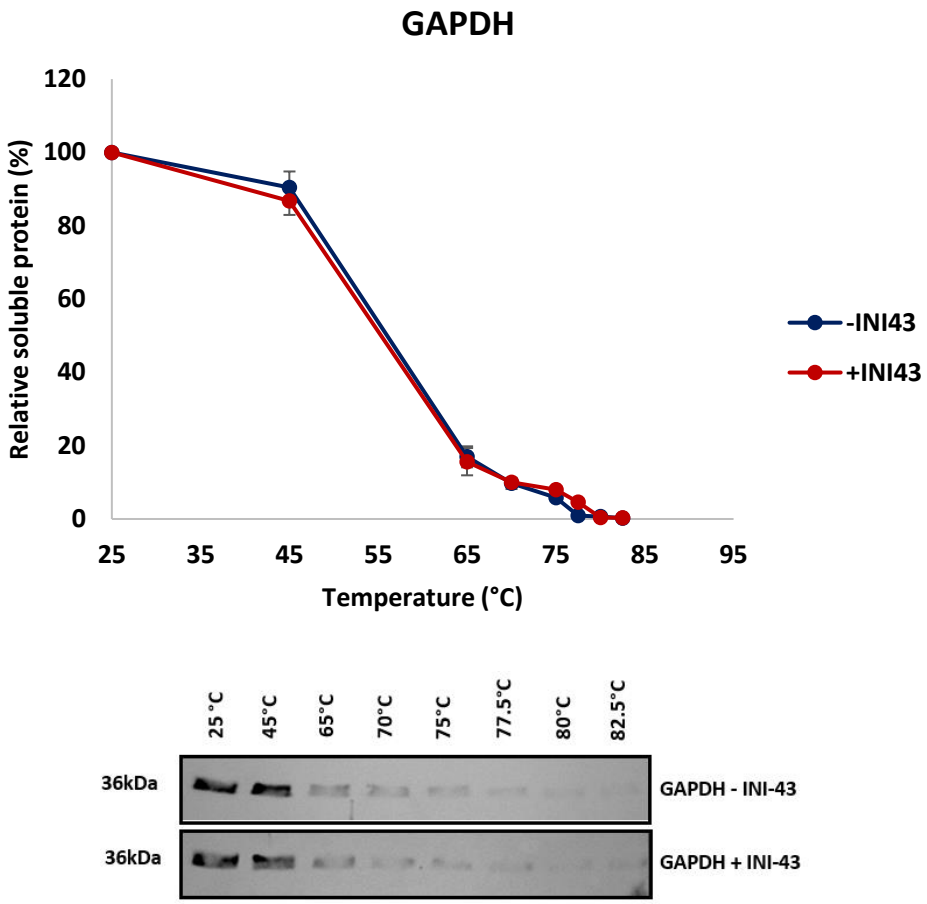

Figure 4.7. Thermal melt curve for GAPDH (control) showing no association with INI-43 in intact HeLa cells. HeLa cells were treated with 10 µM of INI-43 for 3 hours and treated at different temperatures. Relative soluble protein (%) was calculated as each band expressed relative to the 25°C band on each respective blot. Representative immunoblot is shown below the respective protein curve. Result shown is the mean ± SEM of experiments performed two independent times. Significance could not be calculated for these experiments as they were performed two independent times.

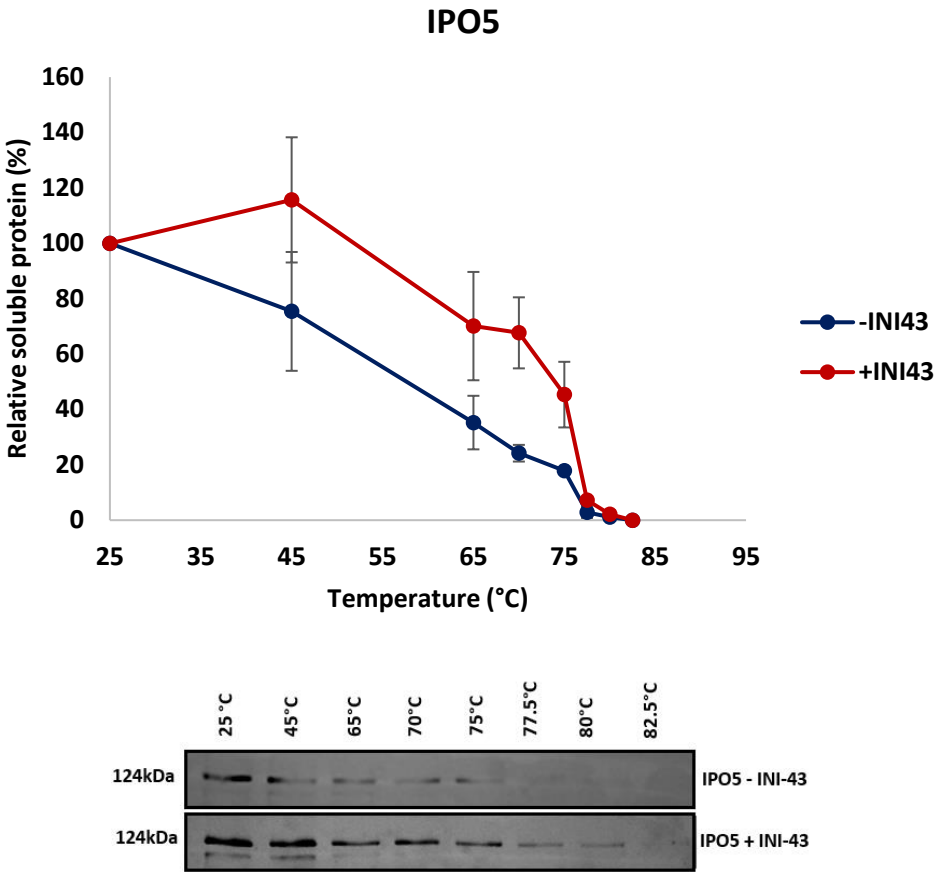

Figure 4.8. Thermal melt curve for IPO5 showing association with INI-43 in intact HeLa cells. HeLa cells were treated with 10 µM of INI-43 for 3 hours and lysates treated at different temperatures. Relative soluble protein (%) was calculated as each band expressed relative to the 25°C band on each respective blot. Representative immunoblot is shown below the protein curve. Result shown is the mean ± SEM of experiments performed two independent times. Significance could not be calculated for these experiments as they were performed two independent times.

4.3 Discussion

In this chapter, we determined that INI-43 has a stabilising effect on KPNβ1, suggesting that it engages with and likely physically binds to KPNβ1. Furthermore, we obtained data to show that INI-43 does not appear to bind to other nuclear transport proteins that are associated with cancer, including CAS, CRM1, KPNα2, TNPO1 and GAPDH (control). Interestingly, we also found that INI-43 appears to bind to the nuclear import protein, IPO5.

There are relatively few studies investigating drug interactions that use CETSA as this is a relatively new technique. However, compared to other available high-throughput screening methodologies and biophysical assays such as Circular Dichroism (CD) and Isothermal Titration Calorimetry (ITC), CETSA is of interest due to its ability to assess protein-ligand interactions inside living cells in their natural physiological context, without the need for any protein modifications, such as labelling, purification or protein engineering. Additionally, CETSA may be applied as a generic tool in the drug screening process as it may provide a chemical starting point and help to remove off-target compounds very quickly early on in the screening process (97). In the present literature, some studies have successfully used CETSA to validate target engagement; Yuan et al. (2021) used CETSA to show that Cucurbitacin B (CuB), a natural bioactive product exerted anti-tumour effects in non-small cell lung cancer (NSCLC) by directly binding to Toll-like receptor 4 (TLR4), which eventually leads to pyroptosis, a type of programmed cell death (98). Luo et al. (2022) also showed that Celastrol, a natural bioactive compound induces ferroptosis, a form of regulated cell death, in activated hepatic stellate cells (HSCs) where Celastrol was shown to directly bind to peroxiredoxins (PRDXs), including PRDX1, PRDX2, PRDX4 and PRDX6 using CETSA (99). Therefore, CETSA is becoming an increasingly popular methodology because it is efficient for assessing target engagement in living cells and tissues, and can be a robust tool in preclinical and clinical drug development.

To our knowledge, this is the first study using CETSA to show that INI-43 binds to KPNβ1, in cervical cancer cells. Previous work performed in our laboratory used purified protein and the biophysical assays Circular Dichroism (CD) and Isothermal Titration Calorimetry (ITC) to show that INI-43 interacts with KPNβ1 (Erin Strydom, PhD thesis, 2016). This study together with

the results presented here using endogenous drug : protein interactions inside living cells, support that INI-43 engages with KPNβ1 as a target. Our results suggest that INI-43 targets KPNβ1 inside living cells and stabilises the protein complex and in this manner correlates with its cytotoxic effects. INI-43 was identified as a drug that targets KPNβ1 in the overlapping Ran and KPNα2 binding sites, as these were the sites shown to be required in the nuclear import process (70). Therefore, it would be of interest to investigate the exact regions that INI-43 binds to on KPNβ1 using X-ray crystallography, or by mutating certain regions on the protein and monitoring drug : protein interactions.

Interestingly, we found that INI-43 binds to another Karyopherin protein, IPO5. IPO5 is a nuclear import protein that transports cargoes with a nuclear localisation signal (NLS) from the cytoplasm into the nucleus by a Ran-dependent mechanism (100). KPNβ1 is a protein that similarly transports NLS-containing cargoes via a Ran-dependent mechanism. Therefore, we hypothesise that KPNβ1 and IPO5 may have structural similarities allowing for INI-43 interactions. Interestingly, IPO5, like KPNβ1, has been previously identified to be upregulated in cancer and associated with cancer development (96). Its inhibition using shRNA has been shown to inhibit the growth and migration of colorectal cancer cells (102). If INI-43 does indeed engage with IPO5, as suggested in these preliminary investigations, it is possible that IPO5 inhibition might be a contributing factor towards the anti-cancer effects of INI-43. It is interesting that CRM1 and TNPO1, which are also KPNβ1 homologues, do not appear to interact with INI-43 (103). It would be noteworthy to examine the localisation of CRM1, TNPO1 and IPO5 cargoes after INI-43 treatment, to gain further clarity on the impact of INI-43 on nuclear transport mechanisms in the cell.

Chapter 5

Conclusion

Cancer progression is characterised by several dysregulated molecular events that take place within a cell. In recent years, studies have shown that the expression of members of the Karyopherin protein family is dysregulated in several cancer types, making them potential therapeutic targets in anti-cancer treatment. Interestingly, there is growing evidence of the nuclear import protein, KPNβ1, being overexpressed in several cancer types, including cervical cancer, breast cancer, gastric cancer, amongst others (6,27,30). Therefore, this study set out to investigate the potential targeted inhibition of KPNβ1 as an anti-cancer therapy on a selected panel of cancer types. We investigated the effect of inhibiting KPNβ1 *in vitro* using the small molecule inhibitor, INI-43 that has previously been shown to inhibit KPNβ1-associated nuclear import pathways (70). We further investigated the specificity of INI-43 for KPNβ1 inside cervical cancer cells.

In this study, we report that the KPNβ1 gene and protein is overexpressed in different cancer types compared to normal including cervical cancer, liver cancer, oesophageal cancer, amongst others, corroborating published studies. Furthermore, using patient data from KM Plotter, we show that there is an association between KPNβ1 expression and patient survival in multiple cancer types, including liver cancer, thyroid cancer and lung adenocarcinoma, amongst others. To our knowledge, our study is a first to report such an association in multiple cancer types in one study. Previous studies have shown an association between high KPNβ1 expression and patient survival in other cancer types, for example Hazawa et al. (2020) identified a correlation between high KPNβ1 expression and poorer patient survival in head and neck squamous cell carcinoma and Yang et al. (2022) found that melanoma patients with higher expression of KPNβ1 had poorer survival (104,105). These findings highlight that cancer cells are more dependent on KPNβ1 pathways than non-cancer cells, and that KPNβ1 may be a potential cancer prognostic and diagnostic marker.

Due to its overexpression in cancer, recent studies have suggested that inhibition of KPNβ1 could be a potential anti-cancer strategy. To investigate its application as a therapeutic target, we used the small molecule inhibitor, INI-43 which was identified through *in silico* screening and computationally designed to target KPNβ1 (70). We found that the cancer cells from different tissue origin were more sensitive to INI-43 treatment compared to the non-cancer cell line, ARPE-19. Treatment with INI-43 resulted in cancer cell death via apoptosis at concentrations that had little or no effect on the non-cancer cell line. The CC_{50} value of ARPE-19 was at least two-fold higher than the CC_{50} values of majority of the cancer cell lines, highlighting the increased sensitivity of cancer cells to KPNβ1 inhibition and thereby emphasising the increased reliance of cancer cells on KPNβ1 associated functions. To date, very few inhibitors of KPNβ1 have been identified even though it has been shown to be a promising therapeutic target in anti-cancer treatment. Our results suggest that INI-43 has potential as a pan-cancer inhibitor. Furthermore, we also show that treatment with INI-43 results in cell death via apoptosis in cancers of different origin. This is in line with findings of other studies showing that inhibiting KPNβ1 with siRNA results in cancer cell death by apoptosis (6). A study done using glioblastoma cells showed that inhibition of KPNβ1 upregulated Puma and Noxa and downregulated Mcl-1, leading to the accumulation of Bax and Bak which eventually caused mitochondrial outer membrane permeabilization (MOMP) and leakage of cytochrome c into the cytosol, triggering apoptosis (33). In our laboratory using cervical cancer cells, KPNβ1 inhibition upregulated Noxa and resulted in greater degradation of Mcl-1. This led to mitochondrial membrane permeabilization, releasing cytochrome c and activating caspases triggering apoptosis (100).However, in these studies, INI-43 was not used in the inhibition of KPNβ1 and it would be interesting to determine if the mechanism of apoptotic cell death by INI-43 treatment follows the same mechanism as that observed using siRNA.

In our study, we obtained novel data reporting that INI-43 exerts its inhibitory effects by binding KPNβ1 in intact cervical cancer cells, using the Cellular Thermal Shift Assay (CETSA). This is a relatively new technique that studies target engagement in a biologically relevant environment. It is important that INI-43 binds to KPNβ1, as hypothesised, because binding of a drug to any off-target proteins may lead to unwanted side effects. Using CETSA, we obtained

preliminary evidence that INI-43 engages with KPNβ1 and not with other members of the Karyopherin protein family, including CAS, CRM1, KPNα2, TNPO1 and GAPDH (control) in cervical cancer cell lines providing a measure of confidence in the specificity of INI-43. This however does not exclude that INI-43 may interact with other proteins. Indeed, we found that INI-43 binds to another protein in the Karyopherin family, IPO5. This is also a nuclear import protein, therefore, we hypothesise that IPO5 may have structural similarities to the region of KPNβ1 to which INI-43 binds, particularly since both proteins bind the small GTPase Ran, however, this needs to be further investigated. It would be interesting to determine if INI-43 binds to any other proteins in the whole proteome to further confirm the specificity of INI-43. This can be carried out by combining Mass Spectrometry with CETSA (MS-CETSA), to examine all the interactions (if any) between INI-43 and other proteins in the proteome, forming the basis of future research in our laboratory (101).

In summary, this study set out to determine the pan-cancer effect of INI-43 treatment and to obtain data on INI-43 binding or target engagement in cells. We show that KPNβ1 is overexpressed in many different cancer types compared to normal tissue, highlighting that KPNβ1 may serve as a marker in targeted anti-cancer therapy and in predicting the clinical outcome of patient survival. Our data using *in vitro* cell culture models provides evidence for INI-43 to be used as a pan-cancer therapeutic, broadening its application as an anti-cancer drug with potential to be considered in the drug development pipeline.

5.1 Limitations and future perspectives

In this study, we used different online platforms for bioinformatic analysis such as KM Plotter, which harbours patient data from different databases, therefore, leading to some level of variability as different online platforms contain varying sets of data from different patients. Despite obtaining data from multiple databases to reduce variability, it should be kept in mind that results may still vary due to cancer heterogeneity.

The cytotoxic effects of INI-43 as a pan-cancer therapeutic agent in this study was done using cell lines (cancer and non-cancer) grown in tissue culture conditions. The use of cell lines has certain limitations as their ability to be grown outside of a living organism can give rise to alterations in cellular behaviour which may differ to that in a living organism where the cellular microenvironment is important for cellular processes. Cell lines, however, are traditionally used as initial experimental models in proof of principal experiments. Future work will include determining the pan-cancer effect of INI-43 using *in vivo* mouse models, which in itself has limitations.

This study obtained evidence that INI-43 interacts with KPNβ1. However, the CETSA experiments suggesting that INI-43 also interacts with IPO5 were only carried out two independent times due to time limitations in the course of this Master's study. Therefore, to obtain more conclusive data that is statistically significant for IPO5 and other proteins included in the study, the experiments would need to repeated. In addition, future prospects include determining if INI-43 binds to other proteins in the proteome to rule out effects from any off-target binding, by combining Mass Spectrometry with CETSA (MS-CETSA). Additionally, it would be interesting to investigate the exact regions that INI-43 binds to on KPNβ1 using X-ray crystallography, or by mutating certain regions on the protein and monitoring drug : protein interactions

Appendix I- Solutions

Tissue culture solutions:

Trypsin-EDTA
0.5 g Trypsin
1.45 g $Na_2HPO_4.2H_2O$
8 g NaCl
0.2 g $KHPO_4$
0.2 g KCL
10 mM EDTA, pH 8
Make up to 1L with PBS

Cell- freezing Media
90% Complete Media
10% DMSO

MTT reagent (5 mg/ml)
100 mg MTT
20 ml PBS
Vortex and incubate at 37˚C in a water bath for 15 minutes
Filter using a 0.22 µm filter
Store at 4˚C in the dark by wrapping in foil for up to one month

Solubilisation Reagent
25 g SLS
Up to 250 ml with dH_2O
76.6 µl concentrated HCl

Protein solutions:

RIPA buffer
150 mM NaCl
1% Triton-X-100
1% Sodium Deoxycholate
0.1% SDS
10 mM Tris-Cl pH 7.5
Store in fridge at 4˚C

CETSA lysis buffer
100 mM Ammonium Sulfate
400 mM NaCl
10% Glycerol
0.5% n-Dodecyl b-D-maltoside (DDM)
Store in fridge at 4˚C

10X PBS
40 g NaCl
1 g KCl
3.82 g $Na_2HPO_4.2H20$
1 g KH_2PO_4
Make up to 500 ml with dH_20

1M Tris-Cl (pH 6.8)
24.23 g Tris
200 ml dH_2O
Adjust pH to 6.8 using concentrated HCl
Make up to 200 ml with dH_2O

1M Tris-Cl (pH 8.8)
24.23 g Tris
200 ml dH2O
Adjust pH to 8.8 using concentrated HCl
Make up to 200 ml with dH_2O

Western blot solutions:

4% Stacking Gel
3.65 ml dH_20
0.625 ml 1M Tris-Cl (pH 6.8)
50 µl 10% SDS
0.650 ml 30% Acrylamide
60 µl 10% APS
6 µl TEMED

10% Separating Gel
2.75 ml dH_20
3.75 ml 1M Tris-Cl (pH 8.8)
100 µl 10% SDS
3.35 ml 30% Acrylamide
200 µl 10% APS
20 µl TEMED

15% Separating Gel
3.3 ml dH_20
3.9 ml 1M Tris-Cl (pH 8.8)
150 µl 10% SDS
7.5 ml 30% Acrylamide
150 µl 10% APS
15 µl TEMED

Loading dye (4 X)
2.5 ml 1M Tris-Cl (pH 6.8)
3 ml 20% SDS
0.5 ml 0.1% Bromophenol Blue
4 ml Glycerol
1 ml 100% β-mercaptoethanol

10 X Running Buffer
20 g Glycine
31.6 g Tris
50 ml 10% SDS
Up to 500 ml with dH_2O

1 X Running Buffer
100 ml 10 X running buffer
900 ml dH_2O

10 X Transfer Buffer
72 g Glycine
19 g Tris
Up to 500 ml with dH_2O

1 X Transfer Buffer
200 ml Isopropanol
100 ml 10 X Transfer
700 ml dH_20

10 X TBS
24.23 g Tris
80.06 g NaCl
Add 800 ml dH_2O
Adjust pH to 7.6 using concentrated HCl
Volume made up to 1L using dH_2O

1 X TBST
100 ml 10 X TBS
900 ml dH_2O
1 ml Tween-20

5% milk powder
1 g milk
20 ml TBST

10% APS
1 g APS
10ml dH_2O

Appendix II – Protein ladders

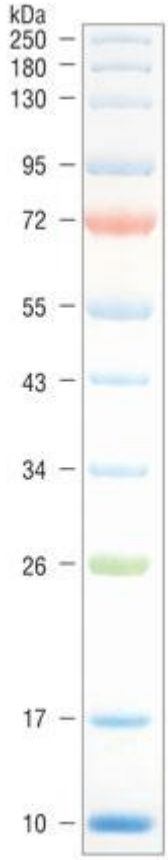

Figure A1.1 Colour Prestained Protein Standard, Broad Range (10-250 kDa). Protein ladder (BioLabs, New England) used during Western Blot analysis. 5 µl of protein ladder was used to determine size of protein bands on 10% SDS-PAGE gels.

References

1. Corrie PG. Cytotoxic chemotherapy: clinical aspects. Medicine (Baltimore). 2008 Jan;36(1):24–8.

2. Nygren P. What is cancer chemotherapy? Acta Oncol. 2001 Jan 1;40(2–3):166–74.

3. Partridge AH, Burstein HJ, Winer EP. Side effects of chemotherapy and combined chemohormonal therapy in women with early-stage breast cancer. J Natl Cancer Inst Monogr. 2001;(30):135–42.

4. Baudino TA. Targeted Cancer Therapy: The Next Generation of Cancer Treatment. Curr Drug Discov Technol. 2015;12(1):3–20.

5. Lee YT, Tan YJ, Oon CE. Molecular targeted therapy: Treating cancer with specificity. Eur J Pharmacol. 2018 Sep;834:188–96.

6. van der Watt PJ, Maske CP, Hendricks DT, Parker MI, Denny L, Govender D, et al. The Karyopherin proteins, Crm1 and Karyopherin β1, are overexpressed in cervical cancer and are critical for cancer cell survival and proliferation. Int J Cancer. 2009 Apr 15;124(8):1829–40.

7. Nigg EA. Nucleocytoplasmic transport: signals, mechanisms and regulation. Nature. 1997 Apr 24;386(6627):779–87.

8. Neumann N, Lundin D, Poole AM. Comparative Genomic Evidence for a Complete Nuclear Pore Complex in the Last Eukaryotic Common Ancestor. PLoS ONE. 2010 Oct 8;5(10):e13241.

9. Grossman E, Medalia O, Zwerger M. Functional Architecture of the Nuclear Pore Complex. Annu Rev Biophys. 2012 Jun 9;41(1):557–84.

10. Çağatay T, Chook YM. Karyopherins in cancer. Curr Opin Cell Biol. 2018 Jun 1;52:30–42.

11. Tran EJ, Wente SR. Dynamic nuclear pore complexes: life on the edge. Cell. 2006 Jun 16;125(6):1041–53.

12. Freitas N, Cunha C. Mechanisms and Signals for the Nuclear Import of Proteins. Curr Genomics. 2009 Dec;10(8):550–7.

13. Mosammaparast N, Pemberton LF. Karyopherins: from nuclear-transport mediators to nuclear-function regulators. Trends Cell Biol. 2004 Oct;14(10):547–56.

14. Fukuda M, Asano S, Nakamura T, Adachi M, Yoshida M, Yanagida M, et al. CRM1 is responsible for intracellular transport mediated by the nuclear export signal. Nature. 1997 Nov 20;390(6657):308–11.

15. Hall MN, Corbett AH, Pavlath GK. Regulation of nucleocytoplasmic transport in skeletal muscle. Curr Top Dev Biol. 2011;96:273–302.

16. Lau CK, Delmar VA, Chan RC, Phung Q, Bernis C, Fichtman B, et al. Transportin regulates major mitotic assembly events: from spindle to nuclear pore assembly. Mol Biol Cell. 2009 Sep;20(18):4043–58.

17. Harel A, Chan RC, Lachish-Zalait A, Zimmerman E, Elbaum M, Forbes DJ. Importin β Negatively Regulates Nuclear Membrane Fusion and Nuclear Pore Complex Assembly. Mol Biol Cell. 2003 Nov;14(11):4387–96.

18. Ishizawa J, Kojima K, Hail N, Tabe Y, Andreeff M. Expression, function, and targeting of the nuclear exporter chromosome region maintenance 1 (CRM1) protein. Pharmacol Ther. 2015 Sep;153:25–35.

19. Aggarwal A, Agrawal DK. Importins and Exportins Regulating Allergic Immune Responses. Mediators Inflamm. 2014;2014:476357.

20. Stelma T, Chi A, van der Watt PJ, Verrico A, Lavia P, Leaner VD. Targeting nuclear transporters in cancer: Diagnostic, prognostic and therapeutic potential. IUBMB Life. 2016 Apr;68(4):268–80.

21. Kuusisto HV, Wagstaff KM, Alvisi G, Roth DM, Jans DA. Global enhancement of nuclear localization-dependent nuclear transport in transformed cells. FASEB J Off Publ Fed Am Soc Exp Biol. 2012 Mar;26(3):1181–93.

22. Wan Y, Wang J, Sun F, Chen M, Hou X, Fang H. Design, synthesis and preliminary biological studies of pyrrolidine derivatives as Mcl-1 inhibitors. Bioorg Med Chem. 2015 Dec 15;23(24):7685–93.

23. van der Watt PJ, Ngarande E, Leaner VD. Overexpression of Kpnβ1 and Kpnα2 importin proteins in cancer derives from deregulated E2F activity. PloS One. 2011;6(11):e27723.

24. Laurila E, Vuorinen E, Savinainen K, Rauhala H, Kallioniemi A. KPNA7, a nuclear transport receptor, promotes malignant properties of pancreatic cancer cells in vitro. Exp Cell Res. 2014 Mar 10;322(1):159–67.

25. Liang XT, Pan K, Chen MS, Li JJ, Wang H, Zhao JJ, et al. Decreased expression of XPO4 is associated with poor prognosis in hepatocellular carcinoma. J Gastroenterol Hepatol. 2011 Mar;26(3):544–9.

26. Melo SA, Moutinho C, Ropero S, Calin GA, Rossi S, Spizzo R, et al. A genetic defect in exportin-5 traps precursor microRNAs in the nucleus of cancer cells. Cancer Cell. 2010 Oct 19;18(4):303–15.

27. Kuusisto HV, Jans DA. Hyper-dependence of breast cancer cell types on the nuclear transporter Importin β1. Biochim Biophys Acta. 2015 Aug;1853(8):1870–8.

28. Kodama M, Kodama T, Newberg JY, Katayama H, Kobayashi M, Hanash SM, et al. In vivo loss-of-function screens identify KPNB1 as a new druggable oncogene in epithelial ovarian cancer. Proc Natl Acad Sci. 2017 Aug 29;114(35):E7301–10.

29. Yang J, Gsuo Y, Lu C, Zhang R, Wang Y, Luo L, et al. Inhibition of Karyopherin beta 1 suppresses prostate cancer growth. Oncogene. 2019 Jun;38(24):4700–14.

30. Zhu J, Wang Y, Huang H, Yang Q, Cai J, Wang Q, et al. Upregulation of KPNβ1 in gastric cancer cell promotes tumor cell proliferation and predicts poor prognosis. Tumour Biol J Int Soc Oncodevelopmental Biol Med. 2016 Jan;37(1):661–72.

31. Sekimoto N, Suzuki Y, Sugano S. Decreased KPNB1 Expression is Induced by PLK1 Inhibition and Leads to Apoptosis in Lung Adenocarcinoma. J Cancer. 2017 Nov 6;8(19):4125–40.

32. Zhang Y, Li KF. Karyopherin β1 deletion suppresses tumor growth and metastasis in colorectal cancer (CRC) by reducing MET expression. Biomed Pharmacother. 2019 Dec 1;120:109127.

33. Zhu ZC, Liu JW, Li K, Zheng J, Xiong ZQ. KPNB1 inhibition disrupts proteostasis and triggers unfolded protein response-mediated apoptosis in glioblastoma cells. Oncogene. 2018;37(22):2936–52.

34. Wang T, Huang Z, Huang N, Peng Y, Gao M, Wang X, et al. Inhibition of KPNB1 Inhibits Proliferation and Promotes Apoptosis of Chronic Myeloid Leukemia Cells Through Regulation of E2F1. OncoTargets Ther. 2019;12:10455–67.

35. Yang F, Li L, Mu Z, Liu P, Wang Y, Zhang Y, et al. Tumor-promoting properties of karyopherin β1 in melanoma by stabilizing Ras-GTPase-activating protein SH3 domain-binding protein 1. Cancer Gene Ther. 2022 Jul 28;1–12.

36. Isali I, McClellan P, Calaway A, Prunty M, Abbosh P, Mishra K, et al. Gene network profiling in muscle-invasive bladder cancer: A systematic review and meta-analysis. Urol Oncol. 2022 May;40(5):197.e11-197.e23.

37. Yang L, Hu B, Zhang Y, Qiang S, Cai J, Huang W, et al. Suppression of the nuclear transporter-KPNβ1 expression inhibits tumor proliferation in hepatocellular carcinoma. Med Oncol Northwood Lond Engl. 2015 Apr;32(4):128.

38. Hazawa M, Yoshino H, Nakagawa Y, Shimizume R, Nitta K, Sato Y, et al. Karyopherin-β1 Regulates Radioresistance and Radiation-Increased Programmed Death-Ligand 1 Expression in Human Head and Neck Squamous Cell Carcinoma Cell Lines. Cancers. 2020 Apr 8;12(4):908.

39. He S, Miao X, Wu Y, Zhu X, Miao X, Yin H, et al. Upregulation of nuclear transporter, Kpnβ1, contributes to accelerated cell proliferation- and cell adhesion-mediated drug resistance (CAM-DR) in diffuse large B-cell lymphoma. J Cancer Res Clin Oncol. 2016 Mar;142(3):561–72.

40. Brinkmann U, Brinkmann E, Gallo M, Scherf U, Pastan I. Role of CAS, a human homologue to the yeast chromosome segregation gene CSE1, in toxin and tumor necrosis factor mediated apoptosis. Biochemistry. 1996 May 28;35(21):6891–9.

41. Shiraki K, Fujikawa K, Sugimoto K, Ito T, Yamanaka T, Suzuki M, et al. Cellular apoptosis susceptibility protein and proliferation in human hepatocellular carcinoma. Int J Mol Med. 2006 Jul;18(1):77–81.

42. Li Y, Yuan S, Liu J, Wang Y, Zhang Y, Chen X, et al. CSE1L silence inhibits the growth and metastasis in gastric cancer by repressing GPNMB via positively regulating transcription factor MITF. J Cell Physiol. 2020 Mar;235(3):2071–9.

43. Stawerski P, Wągrowska-Danilewicz M, Stasikowska O, Danilewicz M. Immunoexpression of CAS protein is augmented in high grade serous ovarian tumors. Pol J Pathol [Internet]. 2011 [cited 2022 Oct 28];61(4). Available from: https://www.termedia.pl/Immunoexpression-of-CAS-protein-is-augmented-in-high-grade-serous-ovarian-tumors,55,16131,1,1.html

44. Stella Tsai CS, Chen HC, Tung JN, Tsou SS, Tsao TY, Liao CF, et al. Serum cellular apoptosis susceptibility protein is a potential prognostic marker for metastatic colorectal cancer. Am J Pathol. 2010 Apr;176(4):1619–28.

45. Liu W, Zhou Z, Li Y, Xu J, Shen Y, Luo S, et al. CSE1L silencing impairs tumor progression via MET/STAT3/PD-L1 signaling in lung cancer. Am J Cancer Res. 2021;11(9):4380–93.

46. Ys W, C P, Y G, Y L. CSE1L promotes proliferation and migration in oral cancer through positively regulating MITF. Eur Rev Med Pharmacol Sci [Internet]. 2020 May [cited 2022 Nov 7];24(10). Available from: https://pubmed.ncbi.nlm.nih.gov/32495878/

47. Chang CC, Tai CJ, Su TC, Shen KH, Lin SH, Yeh CM, et al. The prognostic significance of nuclear CSE1L in urinary bladder urothelial carcinomas. Ann Diagn Pathol. 2012 Oct;16(5):362–8.

48. Wellmann A, Krenacs L, Fest T, Scherf U, Pastan I, Raffeld M, et al. Localization of the cell proliferation and apoptosis-associated CAS protein in lymphoid neoplasms. Am J Pathol. 1997 Jan;150(1):25–30.

49. Zhang X, Zhang X, Mao T, Xu H, Cui J, Lin H, et al. CSE1L, as a novel prognostic marker, promotes pancreatic cancer proliferation by regulating the AKT/mTOR signaling pathway. J Cancer. 2021 Mar 14;12(10):2797–806.

50. Brinkmann U, Brinkmann E, Gallo M, Pastan I. Cloning and characterization of a cellular apoptosis susceptibility gene, the human homologue to the yeast chromosome segregation gene CSE1. Proc Natl Acad Sci U S A. 1995 Oct 24;92(22):10427–31.

51. van der Watt PJ, Zemanay W, Govender D, Hendricks DT, Parker MI, Leaner VD. Elevated expression of the nuclear export protein, Crm1 (exportin 1), associates with human oesophageal squamous cell carcinoma. Oncol Rep. 2014 Aug 1;32(2):730–8.

52. Noske A, Weichert W, Niesporek S, Röske A, Buckendahl AC, Koch I, et al. Expression of the nuclear export protein chromosomal region maintenance/exportin 1/Xpo1 is a prognostic factor in human ovarian cancer. Cancer. 2008 Apr 15;112(8):1733–43.

53. Zhou F, Qiu W, Yao R, Xiang J, Sun X, Liu S, et al. CRM1 is a novel independent prognostic factor for the poor prognosis of gastric carcinomas. Med Oncol Northwood Lond Engl. 2013 Dec;30(4):726.

54. Gousias K, Niehusmann P, Gielen GH, Simon M. Karyopherin a2 and chromosome region maintenance protein 1 expression in meningiomas: novel biomarkers for recurrence and malignant progression. J Neurooncol. 2014 Jun;118(2):289–96.

55. ÖZDAŞ S, ÖZDAŞ T. Crm1 knockdown by specific small interfering RNA reduces cell proliferation and induces apoptosis in head and neck cancer cell lines. Turk J Biol. 2018 Apr 27;42(2):132–43.

56. Huang W yi, Yue L, Qiu W shen, Wang LW, Zhou X han, Sun Y jue. Prognostic value of CRM1 in pancreas cancer. Clin Investig Med Med Clin Exp. 2009 Dec 1;32(6):E315.

57. Yao Y, Dong Y, Lin F, Zhao H, Shen Z, Chen P, et al. The expression of CRM1 is associated with prognosis in human osteosarcoma. Oncol Rep. 2009 Jan;21(1):229–35.

58. Kojima K, Kornblau SM, Ruvolo V, Dilip A, Duvvuri S, Davis RE, et al. Prognostic impact and targeting of CRM1 in acute myeloid leukemia. Blood. 2013 May 16;121(20):4166–74.

59. Sakai M, Sohda M, Miyazaki T, Suzuki S, Sano A, Tanaka N, et al. Significance of karyopherin-{alpha} 2 (KPNA2) expression in esophageal squamous cell carcinoma. Anticancer Res. 2010 Mar;30(3):851–6.

60. Alshareeda AT, Negm OH, Green AR, Nolan CC, Tighe P, Albarakati N, et al. KPNA2 is a nuclear export protein that contributes to aberrant localisation of key proteins and poor prognosis of breast cancer. Br J Cancer. 2015 Jun 9;112(12):1929–37.

61. Altan B, Yokobori T, Mochiki E, Ohno T, Ogata K, Ogawa A, et al. Nuclear karyopherin-α2 expression in primary lesions and metastatic lymph nodes was associated with poor prognosis and progression in gastric cancer. Carcinogenesis. 2013 Oct;34(10):2314–21.

62. Zheng M, Tang L, Huang L, Ding H, Liao WT, Zeng MS, et al. Overexpression of karyopherin-2 in epithelial ovarian cancer and correlation with poor prognosis. Obstet Gynecol. 2010 Oct;116(4):884–91.

63. Jiang P, Tang Y, He L, Tang H, Liang M, Mai C, et al. Aberrant expression of nuclear KPNA2 is correlated with early recurrence and poor prognosis in patients with small hepatocellular carcinoma after hepatectomy. Med Oncol Northwood Lond Engl. 2014 Aug;31(8):131.

64. Wang CI, Wang CL, Wang CW, Chen CD, Wu CC, Liang Y, et al. Importin subunit alpha-2 is identified as a potential biomarker for non-small cell lung cancer by integration of the cancer cell secretome and tissue transcriptome. Int J Cancer. 2011 May 15;128(10):2364–72.

65. Grupp K, Habermann M, Sirma H, Simon R, Steurer S, Hube-Magg C, et al. High nuclear karyopherin α 2 expression is a strong and independent predictor of biochemical recurrence in prostate cancer patients treated by radical prostatectomy. Mod Pathol Off J U S Can Acad Pathol Inc. 2014 Jan;27(1):96–106.

66. Jensen JB, Munksgaard PP, Sørensen CM, Fristrup N, Birkenkamp-Demtroder K, Ulhøi BP, et al. High expression of karyopherin-α2 defines poor prognosis in non-muscle-invasive bladder cancer and in patients with invasive bladder cancer undergoing radical cystectomy. Eur Urol. 2011 May;59(5):841–8.

67. Winnepenninckx V, Lazar V, Michiels S, Dessen P, Stas M, Alonso SR, et al. Gene expression profiling of primary cutaneous melanoma and clinical outcome. J Natl Cancer Inst. 2006 Apr 5;98(7):472–82.

68. Xiang S, Wang Z, Ye Y, Zhang F, Li H, Yang Y, et al. E2F1 and E2F7 differentially regulate KPNA2 to promote the development of gallbladder cancer. Oncogene. 2019 Feb;38(8):1269–81.

69. Shi B, Su B, Fang D, Tang Y, Xiong G, Guo Z, et al. High expression of KPNA2 defines poor prognosis in patients with upper tract urothelial carcinoma treated with radical nephroureterectomy. BMC Cancer. 2015 May 9;15:380.

70. van der Watt PJ, Chi A, Stelma T, Stowell C, Strydom E, Carden S, et al. Targeting the Nuclear Import Receptor Kpnβ1 as an Anticancer Therapeutic. Mol Cancer Ther. 2016 Apr;15(4):560–73.

71. Hintersteiner M, Ambrus G, Bednenko J, Schmied M, Knox AJS, Gstach H, et al. Identification of a small molecule inhibitor of importin beta mediated nuclear import by confocal on-bead screening of tagged one-bead one-compound libraries. ACS Chem Biol. 2010 Oct 15;5(10):967–79.

72. Soderholm JF, Bird SL, Kalab P, Sampathkumar Y, Hasegawa K, Uehara-Bingen M, et al. Importazole, a small molecule inhibitor of the transport receptor importin-β. ACS Chem Biol. 2011 Jul 15;6(7):700–8.

73. Wagstaff KM, Sivakumaran H, Heaton SM, Harrich D, Jans DA. Ivermectin is a specific inhibitor of importin α/β-mediated nuclear import able to inhibit replication of HIV-1 and dengue virus. Biochem J. 2012 May 1;443(3):851–6.

74. Nishio M, Sugimachi K, Goto H, Wang J, Morikawa T, Miyachi Y, et al. Dysregulated YAP1/TAZ and TGF-β signaling mediate hepatocarcinogenesis in Mob1a/1b-deficient mice. Proc Natl Acad Sci U S A. 2016 Jan 5;113(1):E71-80.

75. Molina DM, Jafari R, Ignatushchenko M, Seki T, Larsson EA, Dan C, et al. Monitoring Drug Target Engagement in Cells and Tissues Using the Cellular Thermal Shift Assay. Science. 2013 Jul 5;341(6141):84–7.

76. Mateo J, Ong M, Tan DSP, Gonzalez MA, Bono JS de. Appraising iniparib, the PARP inhibitor that never was--what must we learn? Nat Rev Clin Oncol. 2013 Dec 1;10(12):688–97.

77. Schürmann M, Janning P, Ziegler S, Waldmann H. Small-Molecule Target Engagement in Cells. Cell Chem Biol. 2016 Apr 21;23(4):435–41.

78. Rhodes DR, Yu J, Shanker K, Deshpande N, Varambally R, Ghosh D, et al. ONCOMINE: a cancer microarray database and integrated data-mining platform. Neoplasia N Y N. 2004;6(1):1–6.

79. Kuusisto HV, Wagstaff KM, Alvisi G, Roth DM, Jans DA. Global enhancement of nuclear localization-dependent nuclear transport in transformed cells. FASEB J Off Publ Fed Am Soc Exp Biol. 2012 Mar;26(3):1181–93.

80. CC50 - an overview | ScienceDirect Topics [Internet]. [cited 2023 Nov 26]. Available from: https://www.sciencedirect.com/topics/biochemistry-genetics-and-molecular-biology/cc50

81. Wang Q, Armenia J, Zhang C, Penson AV, Reznik E, Zhang L, et al. Unifying cancer and normal RNA sequencing data from different sources. Sci Data. 2018 Apr 17;5(1):180061.

82. Elmore S. Apoptosis: A Review of Programmed Cell Death. Toxicol Pathol. 2007;35(4):495–516.

83. Caspase-Glo® 3/7 Assay System | Caspase 3 Activity Assay | Apoptosis Detection [Internet]. [cited 2023 Feb 7]. Available from: https://worldwide.promega.com/products/cell-health-assays/apoptosis-assays/caspase_glo-3_7-assay-systems/

84. Muller PY, Milton MN. The determination and interpretation of the therapeutic index in drug development. Nat Rev Drug Discov. 2012 Oct;11(10):751–61.

85. Ferreira BI, Cautain B, Grenho I, Link W. Small Molecule Inhibitors of CRM1. Front Pharmacol. 2020;11:625.

86. Kudo N, Matsumori N, Taoka H, Fujiwara D, Schreiner EP, Wolff B, et al. Leptomycin B inactivates CRM1/exportin 1 by covalent modification at a cysteine residue in the central conserved region. Proc Natl Acad Sci. 1999 Aug 3;96(16):9112–7.

87. Lapalombella R, Sun Q, Williams K, Tangeman L, Jha S, Zhong Y, et al. Selective inhibitors of nuclear export show that CRM1/XPO1 is a target in chronic lymphocytic leukemia. Blood. 2012 Nov 29;120(23):4621–34.

88. Garzon R, Savona M, Baz R, Andreeff M, Gabrail N, Gutierrez M, et al. A phase 1 clinical trial of single-agent selinexor in acute myeloid leukemia. Blood. 2017 Jun 15;129(24):3165–74.

89. Vogl DT, Dingli D, Cornell RF, Huff CA, Jagannath S, Bhutani D, et al. Selective Inhibition of Nuclear Export With Oral Selinexor for Treatment of Relapsed or Refractory Multiple Myeloma. J Clin Oncol Off J Am Soc Clin Oncol. 2018 Mar 20;36(9):859–66.

90. Podar K, Shah J, Chari A, Richardson PG, Jagannath S. Selinexor for the treatment of multiple myeloma. Expert Opin Pharmacother. 2020 Mar;21(4):399–408.

91. Gravina GL, Mancini A, Sanita P, Vitale F, Marampon F, Ventura L, et al. KPT-330, a potent and selective exportin-1 (XPO-1) inhibitor, shows antitumor effects modulating the expression of cyclin D1 and survivin in prostate cancer models. BMC Cancer. 2015 Dec 1;15(1):941.

92. Ishii T, Okai T, Iwatani-Yoshihara M, Mochizuki M, Unno S, Kuno M, et al. CETSA quantitatively verifies in vivo target engagement of novel RIPK1 inhibitors in various biospecimens. Sci Rep. 2017 Oct 12;7(1):13000.

93. Hashimoto M, Girardi E, Eichner R, Superti-Furga G. Detection of Chemical Engagement of Solute Carrier Proteins by a Cellular Thermal Shift Assay. ACS Chem Biol. 2018 Jun 15;13(6):1480–6.

94. Jafari R, Almqvist H, Axelsson H, Ignatushchenko M, Lundbäck T, Nordlund P, et al. The cellular thermal shift assay for evaluating drug target interactions in cells. Nat Protoc. 2014 Sep;9(9):2100–22.

95. cetsa-tbx2-a500_2693745.pdf [Internet]. [cited 2023 Feb 23]. Available from: https://resources.perkinelmer.com/corporate/content/tdlotsheet/cetsa-tbx2-a500_2693745.pdf

96. Martinez NJ, Asawa RR, Cyr MG, Zakharov A, Urban DJ, Roth JS, et al. A widely-applicable high-throughput cellular thermal shift assay (CETSA) using split Nano Luciferase. Sci Rep. 2018 Jun 21;8(1):9472.

97. Axelsson H, Almqvist H, Seashore-Ludlow B, Lundbäck T. Screening for Target Engagement using the Cellular Thermal Shift Assay - CETSA. In: Assay Guidance Manual [Internet] [Internet]. Eli Lilly & Company and the National Center for Advancing Translational Sciences; 2016 [cited 2023 Jul 5]. Available from: https://www.ncbi.nlm.nih.gov/sites/books/NBK374282/

98. Yuan R, Zhao W, Wang QQ, He J, Han S, Gao H, et al. Cucurbitacin B inhibits non-small cell lung cancer in vivo and in vitro by triggering TLR4/NLRP3/GSDMD-dependent pyroptosis. Pharmacol Res. 2021 Aug;170:105748.

99. Luo P, Liu D, Zhang Q, Yang F, Wong YK, Xia F, et al. Celastrol induces ferroptosis in activated HSCs to ameliorate hepatic fibrosis via targeting peroxiredoxins and HO-1. Acta Pharm Sin B. 2022 May;12(5):2300–14.

100. IPO5 - Importin-5 - Homo sapiens (Human) | UniProtKB | UniProt [Internet]. [cited 2023 Apr 3]. Available from: https://www.uniprot.org/uniprotkb/O00410/entry

101. Patouret R. The Nuclear Transport Protein Importin-5: A Promising Target in Oncology and Virology. Chimia. 2021 Apr 28;75(4):319–22.

102. Zhang W, Lu Y, Li X, Zhang J, Lin W, Zhang W, et al. IPO5 promotes the proliferation and tumourigenicity of colorectal cancer cells by mediating RASAL2 nuclear transportation. J Exp Clin Cancer Res CR. 2019 Jul 9;38:296.

103. Khalil B, Chhangani D, Wren MC, Smith CL, Lee JH, Li X, et al. Nuclear import receptors are recruited by FG-nucleoporins to rescue hallmarks of TDP-43 proteinopathy. Mol Neurodegener. 2022 Dec 8;17(1):80.

104. Hazawa M, Yoshino H, Nakagawa Y, Shimizume R, Nitta K, Sato Y, et al. Karyopherin-β1 Regulates Radioresistance and Radiation-Increased Programmed Death-Ligand 1 Expression in Human Head and Neck Squamous Cell Carcinoma Cell Lines. Cancers. 2020 Apr 8;12(4):908.

105. Yang F, Li L, Mu Z, Liu P, Wang Y, Zhang Y, et al. Tumor-promoting properties of karyopherin β1 in melanoma by stabilizing Ras-GTPase-activating protein SH3 domain-binding protein 1. Cancer Gene Ther. 2022 Dec;29(12):1939–50.

106. Angus L, van der Watt PJ, Leaner VD. Inhibition of the nuclear transporter, Kpnβ1, results in prolonged mitotic arrest and activation of the intrinsic apoptotic pathway in cervical cancer cells. Carcinogenesis. 2014 May;35(5):1121–31.

107. Prabhu N, Dai L, Nordlund P. CETSA in integrated proteomics studies of cellular processes. Curr Opin Chem Biol. 2020 Feb;54:54–62.